Anesthetics as Chemical Tools to Study the Structure and Function of Nicotinic Acetylcholine Receptors

Hugo R. Arias* and Pankaj Bhumireddy

Department of Pharmaceutical Sciences, College of Pharmacy, Western University of Health Sciences, 309 E. Second Street, Pomona, CA 91766-1854, USA

Abstract: The nicotinic acetylcholine receptor (AChR) is the archetype of the Cys-loop ligand-gated ion channel receptor superfamily. Noncompetitive antagonists inhibit the AChR without interacting directly with agonist sites. Among non-competitive antagonists, general and local anesthetics have been used for decades to study the structure and function of muscle- as well as neuronal-type AChRs. In this review, we address and update all information regarding the characterization of binding sites and the mechanism of action for n-alkanols, barbiturates, inhalational and dissociative general anesthetics, as well as for tertiary and quaternary local anesthetics. The experimental evidence outlined in this review suggest that: **(1)** several neuronal-type AChRs might be targets for the pharmacological action of distinct anesthetics; **(2)** the molecular components of a specific anesthetic locus on a certain receptor type are different from the structural determinants of the site for the same anesthetic on a different receptor type; **(3)** there are unique binding sites for distinct anesthetics in the same receptor; **(4)** the affinity of a specific anesthetic depends on the AChR conformational state; **(5)** anesthetics may inhibit AChRs by different mechanisms including open-channel-blocking, augmenting the desensitization process, and/or inactivating the opening of resting receptors; and **(6)** some anesthetics may potentiate AChR activity.

I. INTRODUCTION

The muscle-type nicotinic acetylcholine receptor (AChR) is the archetype of the Cys-loop ligand-gated ion channel (LGIC) receptor superfamily which also includes the neuronal-type AChR as well as type A and C γ-aminobutyric acid ($GABA_AR$ and $GABA_CR$), glycine (GlyR), and type 3 5-hydroxytryptamine ($5\text{-}HT_3R$) receptors (reviewed in [1,2]). A scheme of the primary, tertiary, and quaternary structural features of the Cys-loop LGIC superfamily is shown in [Fig. **(1)**].

These different receptors are considered a superfamily because a high degree (30-70%) of homology between the amino acid sequence of each receptor subunit exists [Fig. **(1A)**] (reviewed in [3]). A second characteristic, shared by all members of this LGIC superfamily, is that each subunit can be divided in three domains: **(1) an extracellular domain:** the NH_2-terminal hydrophilic extracellular portion bears the neurotransmitter binding sites and several glycosylation sites. Details of the neurotransmitter binding site for the AChR have been revealed at near atomic resolution using the molluscan acetylcholine (ACh)-binding protein (AChBP) [4,5]. Molecular modeling of the extracellular portion of both the α7 AChR [6] and several $GABA_ARs$ [7] has recently been published. For instance, these studies have determined that each ACh binding site is located at the interface of two subunits (reviewed in [1,5,8]). In addition, a 15-residue Cys-loop exists in the amino terminal, which gives the name to this receptor superfamily; **(2) a transmembrane domain:** each subunit is formed by four highly hydrophobic segments designated M1, M2, M3, and M4 [Fig. **(1B)**]. The membrane-spanning region has a dimension of 30-35 Å (40 Å including the phospholipid headgroup portion). There is now considerable evidence supporting an α-helix secondary structure for these transmembrane segments. The segments M1, M2, and M3 are separated from each other by short hydrophilic stretches. Homologous faces of the five M2 segments, one from each receptor subunit, form the walls of the ion channel. The ion channels from $GABA_AR$, $GABA_CR$, and GlyRs, are permeable to anions (e.g., Cl^- and HCO_3^-), whereas the ion channels from $5\text{-}HT_3R$ and AChRs allow the passage of cations (e.g., Na^+, K^+, and Ca^{2+}). An excellent review on ion selectivity mechanisms has been recently published [8]. The M1, M3, and in particular the M4 transmembrane segment of the AChR are in contact with the lipid membrane; and **(3) a cytoplasmic domain** [Fig. **(1B)**]: this hydrophilic portion is approximately four-fold smaller than the NH_2-terminal domain, and it is located between segments M3 and M4. The M4 segment orientates the COOH-terminus to the synaptic side of the membrane. The large cytoplasmic domain of these receptors carries several phosphorylation sites that modulate receptor function (reviewed in [9]). This domain is involved in biosynthesis, assembly, transport, clustering, and anchoring of these receptors as well.

Information on the structure of LGIC superfamily members has come predominantly from studies of the muscle-type AChR. The muscle-type AChR is a heteropentameric membrane-embedded protein formed by four distinct subunits. The adult muscle-type AChR is in the stoichiometric ratio of $\alpha 1_2\beta 1\varepsilon\delta$, whereas the combination $\alpha 1_2\beta 1\gamma\delta$ predominates in embryonic or denervated muscle as well as in electric organs from *Torpedo* and *Electrophorus* species. Based upon the presence of two adjacent Cys residues at or

*Address correspondence to this author at the Department of Pharmaceutical Sciences, College of Pharmacy, Western University of Health Sciences, 309 E. Second Street, Pomona, CA 91766-1854, USA; Tel: (909) 469-5424; Fax: (909) 469-5600; E-mail: harias@westernu.edu

1389-2037/05 $50.00+.00

close to position 192 and 193 of the *Torpedo* α1 subunit, which participate in agonist/competitive antagonist binding, the neuronal-type AChR subunit classes are designated α (if they contain both Cys residues) and non-α or β (if they do not contain those Cys residues). To date, nine neuronal α subunits (α2 to α10) and three β subunits (β2 to β4) have been identified in vertebrates (reviewed in [1,2,10]).

By homology with the muscle-type AChR, neuronal AChRs are also believed to form oligomers composed of five subunits [11]. Depending on the tissue of origin, AChRs can be combined in several subunit arrangements. There is evidence supporting the existence of neuronal receptors containing one, two, three, or even four different subunits (reviewed in [1,10,12]). Among homomeric receptors, there are α7, α8 (identified only in avian species), and α9 receptors. Heteromeric receptors have two nonequivalent agonist/competitive antagonist binding sites, whereas homomeric receptors [13] see [Fig. **(1C)**] as well as AChBP [4] may have up to five sites. The existence of a high number of structurally-distinct receptor entities, each with different ligand sensitivities, suggests that each AChR class may have a distinct physiological function (reviewed in [10,14]).

The *Torpedo* AChR is believed to have the α1-γ-α1-δ-β1 subunit anticlockwise arrangement (reviewed in [1,12,15]). Nevertheless, there is no direct evidence indicating the arrangement of neuronal subunits around the ion channel. The organization α4-β2-α4-β2-β2 has been suggested for the predominate AChR subtype present in the rat brain and the arrangement α3-α5-β-α3-β (where β may be only β4 or alternatively β2 or β4) is presumed to exist in chicken ciliary ganglion neurons, (reviewed in [1,12,16]).

Cryo-electron microscopy image analysis at ~4 Å resolution has helped elucidate the overall structure of the *Torpedo* AChR (reviewed in [17,18]). Viewed from the synaptic cleft, the AChR appears as a rosette 70-80 Å in diameter with a central depression 25 Å wide. The five subunits are arranged pseudo-symmetrically around an axis that passes through the ion pore, perpendicular to the plane of the lipid membrane. The observed rosette is formed by the extracellular hydrophilic domain of the receptor containing both the NH_2- and the COOH-terminal [Fig. **(1)**]. The NH_2-terminus of each subunit, formed by approximately 210 amino acids, protrudes ~60 Å toward the synaptic cleft. The observed central depression is the vestibule, a large region located on the extracellular domain of the AChR connecting the extracellular medium with the ion channel proper.

The structure of the ion channel has been studied using different methodological approaches including photoaffinity labeling and site-directed mutagenesis in combination with electrophysiological methods. In a simplistic manner, the ion channel can be considered to be similar to a cylindrical tube with a diameter of 20-25 Å that protrudes along the lipid bilayer see [Fig. **(1B)**]. Although the structural characteristics of the transmembrane portion of the channel have not been resolved in detail, the narrowest portion of the cylinder is considered to have a diameter of 7 Å (reviewed in [17,18]). The observed diameter is large enough to allow the passage of Na^+ or K^+ cations with a single hydration shell. This evidence is in agreement with electron microscopic image analyses at ~4 Å resolution indicating that the closed ion channel has a narrow strip of density no longer than two rings of side-chains thick, the so-called gate (reviewed in [17,18]).

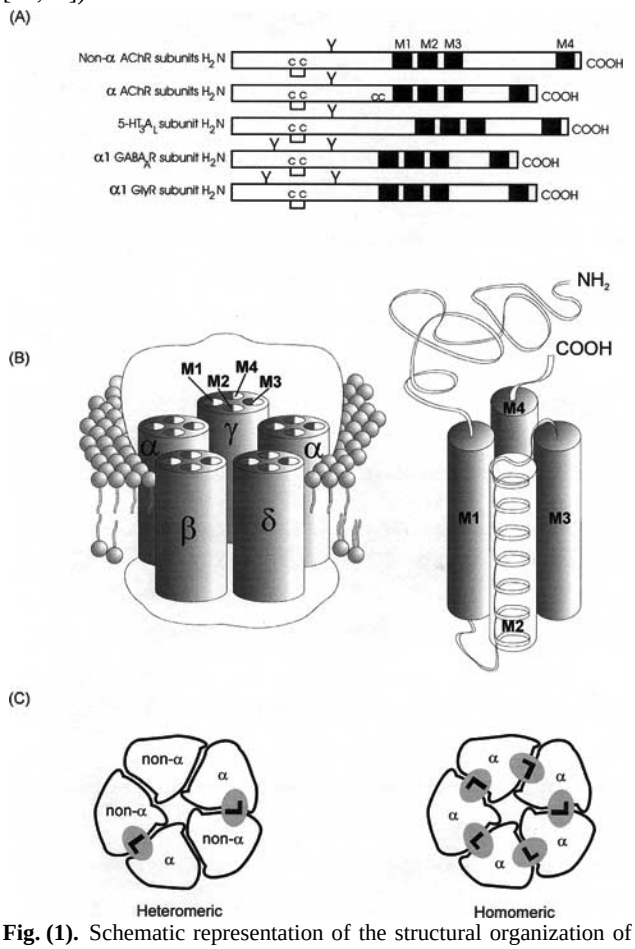

Fig. (1). Schematic representation of the structural organization of the AChR superfamily (modified from [20]). **(A)** Schematic illustration of the primary sequence of several subunits from members of the Cys-loop LGIC superfamily which includes the α (e.g., α1-α10) and non-α (e.g., β1-β4, γ, ε, and δ) subunits of the AChR, the A subunit of the 5-HT_3R, the α1 subunit from the $GABA_A$R, and the α1 subunit from the GlyR. M1-M4, transmembrane domains; C¾C, Cys-Cys bridge found in the LGIC superfamily (homologous to Cys^{128} and Cys^{148} of the α1 AChR subunit); CC, Cys-Cys pair found in the α subunits from both muscle- and neuronal-type AChRs (corresponding to Cys^{192}-Cys^{193} from the α1 AChR subunit); Y, oligosaccharide groups. **(B)** Diagram of the tertiary and quaternary organization of the AChR. Each AChR subunit includes: **(1)** a long NH_2-terminal hydrophilic extracellular domain; **(2)** four highly hydrophobic domains named M1, M2, M3, and M4. It is postulated that the intrinsic ion channel is composed by five M2 segments, one from each subunit. Moreover, M1-M2 and M2-M3 are connected by minor hydrophilic stretches; and **(3)** a major hydrophilic segment facing the cytoplasm. Additionally, the M4 domain orientates the COOH-terminus to the synaptic side of the membrane. **(C)** Schematic representation of the oligomeric organization of AChR. The hypothetical pentameric AChR is formed by two α and three non-α subunits. The two ligand binding sites (L) are located at the interfaces of one α subunit and one non-α chain. Regarding homomeric AChRs (e.g., α7-α9) or for the molluscan AChBP, up to five ligand binding sites may exist.

Additional evidence indicates that there are two categories of domains within the AChR channel (reviewed in [2,19,20]). There is an uncharged domain formed by a series of different rings vectorially disposed from the extracellular to the intracellular channel portion in the order: valine ring (position M2-13), leucine ring (position M2-9), serine ring (position M2-6), and threonine ring (position M2-2). In turn, this uncharged portion is framed by two negatively-charged regions: an anionic ring located at the extracellular portion of the channel [i.e., the outer ring (position M2-20)] and two more anionic rings [i.e., the intermediate ring (position –2) and the inner ring (position –5)] located near the cytoplasmic portion of the channel.

1. Physiological and Pathophysiological Functions of AChRs

At the molecular level, AChRs present a very simple repertoire of functional properties. Several lines of experimental evidence suggest that this receptor classes may exist in a minimum of three interconvertible states (reviewed in [1,2,21]). In the absence of the neurotransmitter ACh, most receptors are in the resting state, a closed but agonist-activatable state. Thus, in the presence of ACh or other agonists, the receptor is activated in the microsecond to millisecond range. This state represents an open ion channel with low affinity for agonists relative to the desensitized state. Upon neurotransmitter binding, the intrinsically-coupled ion channel opens, allowing ions to cross the lipid membrane (i.e., Na^+ and Ca^{2+} enter into the cell whereas K^+ exits the cell), and finally depolarizing the membrane. Membrane depolarization provokes specific physiological responses in the cell. For instance, at the neuromuscular junction, if the membrane depolarization is large enough, an action potential is elicited. This action potential propagates from the neuromuscular junction all over the muscle fiber releasing Ca^{2+} from intracellular stores. The final response in the muscle is the contraction of its myofibrils. In neurons, the excitatory signal provided by the activation of cation channels is summated with other signals, including inhibitory signals such as those provided by the activation of either $GABA_A$Rs or GlyRs, and subsequently re-directed to another neuron or to an endocrine gland cell. In interneurons, activation of AChRs results in inward currents that depolarize the cell increasing the frequency of spontaneous postsynaptic inhibitory currents (reviewed in [16]). Considering that receptors exist on different cell types and AChRs can be located at distinct areas of the same cell, both excitatory and inhibitory activities can be modulated in a complex manner.

Neuronal-type AChRs are involved in higher-order brain mechanisms such as cognition, learning, memory, and behavior, as well as nociception and pain processing (reviewed in [14,16,22,23]). Presynaptic neuronal AChRs are involved in the release of neurotransmitters such as ACh, glutamate, norepinephrine, dopamine, 5-HT, or GABA. Other functions on the peripheral nervous system include auditory function and development, cardiovascular and gastrointestinal actions, muscle contraction and tone. The malfunctioning of these receptors has been considered as the origin of neurological disorders such as Alzheimer's and Parkinson's diseases, nocturnal frontal lobe epilepsy, distinct congenital myasthenic syndromes, schizophrenia, anxiety, depression, chronic pain, as well as drug addiction (reviewed in [14,22-24]).

In the prolonged presence of agonists, the activated receptor converts to a desensitized state. This state is refractory to the pharmacological action of agonists, and the ion channel remains closed. In addition, the desensitized state has high affinity for agonists and some antagonists. After the dissociation of agonist molecules from their binding sites, AChRs in the desensitized state predominantly isomerize directly to the resting state. The physiological role of the desensitization process in the Cys-loop receptor superfamily has thus far not been determined. However, under some pathological conditions the importance of this course of action becomes apparent (reviewed in [25]). For instance, activation and/or subsequent desensitization of neuronal AChR subtypes are believed to underlie behavioral addiction to nicotine (reviewed in [24]).

II. GENERAL ANESTHETICS

An increasing amount of experimental information points to the $GABA_A$R as one of the most important targets to induce general anesthesia. However, several neuronal-type AChRs are considered to be involved in certain additional CNS effects during general anesthesia such as amnesia, lack of attention, behavioral states, and delirium (reviewed in [2,16]). In general, general anesthetics (GAs) act pharmacologically as noncompetitive antagonists (NCAs) on distinct AChRs. In this regard, they can be used as chemical tools to study the structure and function of AChRs.

1. Inhalational General Anesthetics

Several laboratories have shown that a series of inhalational GAs including isoflurane, enflurane, methoxyflurane, halothane, and ether alter the kinetic properties, albeit with distinct patterns, of the muscle-type (embryonic) AChR expressed in the clonal cell line BC_3H-1 at clinical or subclinical doses [26-29]. On the contrary, sevoflurane inhibited embryonic mouse muscle AChR at concentrations higher than clinical doses [30,31]. Interestingly, both mouse and BC_3H-1 muscle receptors showed practically the same sensitivity to isoflurane [29]. Table **1** summarizes the binding and inhibition affinities of inhalational anesthetics for several types of AChRs. Although these studies demonstrated that inhalational anesthetics inhibit AChRs in a noncompetitive manner, there is no clear-cut evidence indicating if this inhibition is mediated by a steric (open-channel-blocking) and/or an allosteric mechanism [28]. For instance, single-channel and macroscopic current analyses suggest that isoflurane and sevoflurane, as well as propofol bind to both open and closed (resting) ion channels with equal affinity [29,30]. In addition, stopped-flow [32] and electrophysiology [27] experiments show that isoflurane increases the apparent affinity of agonists to muscle-type AChRs, suggesting that this GA augmentates the desensitization rate.

In general, neuronal-type AChRs are more sensitive to the action of inhalational anesthetics than muscle-type AChRs (see Table **1**). For example, halothane inhibits different AChRs with the following potencies (IC_{50} values in μM): $\alpha4\beta2$ (27 ± 5) > $\alpha2\beta4$ (47 ± 5) > $\alpha4\beta4$ (105 ± 17) > $\alpha1\beta1\gamma\delta$ (870 ± 50) [31]. The observed Hill coefficients (n_Hs) are

close to unity suggesting one GA binding site per neuronal-type AChR. However, studies on the macroscopic concentration-response curve for isoflurane inhibition of mouse AChR ion channels suggest the existence of more than one binding site [29]. Several anesthetics (e.g., methoxyflurane, methohexital, and etomidate) inhibit the receptors from bovine chromaffin cells, suggesting that these agents mediate postsynaptic sympathetic inhibition by impairing epinephrine release from the adrenal glands [33]. Several volatile anesthetics including isoflurane, enflurane, methoxyflurane, and halothane also inhibit molluscan (ganglionic) AChRs [34].

It has been suggested that appropiate targets for anesthetic action should be affected by anesthetic drugs but not affected by the new class of compounds called "nonimmobilizers" (nonanesthetics) [35]. The fact that nonimmobilizers such as 1,2-dichlorohexafluorocyclobutane and 2,3-dichlorooctafluorobutane have very little effect if any on several neuronal-type AChRs (e.g., α2β4, α3β4, and α4β2) suggests that these receptors might be involved in the mechanisms of general anesthesia [36].

Interestingly, α4- [37] and α3-containing receptors [38] are more sensitive to the action of GAs than α7 receptors [39] (see Table **1**). Since the isoflurane-induced inhibition of the α7 receptor result was similar to that using receptor chimeras formed by the amino-terminal portion from the α7 receptor and the remainder from the 5-HT_3R (see Table **1**), the authors concluded that the GA binding domain should be located at the amino-terminal domain of the α7 receptor [39]. This conclusion correlates very well with that for the localization of the ethanol binding site on the same receptor class [40] (see section II.2.b.). Using homomeric α3/α7 chimeras, an additional site that modulates (but does not participate directly in) halothane sensitivity was located at the M2-M3 extracellular loop [38]. More specifically, muations $Ile^{263}Met$ and $Val^{269}Ser$ in the chimera affected halothane sensitivity.

One possible way to explain the mechanism of action of GAs on AChRs is to determine its site(s) of action on the protein by site-directed mutagenesis in combination with electrophysiological recordings. This approach has helped to demonstrate the existence of an inhibitory site for isoflurane in the M2 transmembrane segment of the muscle-type AChR ion channel. More specifically, the double (because there are two α1 subunits) $\alpha1Ser^{252}Ile$ [41] and triple $\alpha1Ser^{252}Ala/\beta1Thr^{263}Ala$ mutation [29], which are located at position M2-10, but not $\alpha1Ser^{248}Ala/\delta Thr^{264}Ala$ that is located at position M2-6 (serine ring), increased the sensitivity of the muscle AChR to isoflurane (see Table **1**). Interestingly, this site correlates very well with the inhibitory site for long-alcohols (see section II.2.a). The above results suggest that the decrease in polarity provided by Ala mutations at position M2-10 increases isoflurane affinity for the resting (closed) state without changing the affinity for the open state. Two other GAs, ether and propofol, also present higher affinity for closed AChRs. In contrast, isoflurane has no preference for the different conformational states of the wild-type AChR. The binding site for the local anesthetic (LA) QX-222 is located between position M2-6 and M2-10 (see section III.2.a.). Nevertheless the inhibitory action of isoflurane, ether, or propofol was not changed by mutations at position M2-6. Thus, the GA binding domain partially overlaps the QX-222 locus. Since QX-222 prefers the open channel, the aromatic moiety of the LA and isoflurane should interact distinctly with residues at position M2-10. This idea is consistent with the results from Dilger and Vidal [26] indicating that ether stabilizes QX-222 binding. A plausible localization for the isoflurane binding site that includes the valine ring (position M2-13) was hypothesized by Barann *et al.* [42]. The fact that mutations on $\beta2Val^{253}$, $\beta4Phe^{255}$, and $\alpha4Val^{254}$, which are homologous residues at position M2-13, determine isoflurane sensitivity but do not form its binding site [43], does not support the above hypothesis. Thus, more experimental data will be necessary to clarify this issue.

Another approach that has been used to localize inhalational anesthetic binding sites on the AChR is the photoaffinity labeling method. [^{14}C]Halothane was the first GA used for photoaffinity labeling purposes [44]. In this regard, [^{14}C]halothane specifically photoincorporates into purified AChRs with a K_d value of 180 ± 40 μM (see Table **1**) and a stoichiometry of 2.5 ± 0.4 binding sites per AChR. Although isoflurane binds to *Torpedo* AChRs with a similar affinity (see Table **1**), a stoichiometry of 9-10 binding sites per AChR was determined by ^{19}F-NMR spectroscopy and gas chromatography [45]. Interestingly, the motion of isoflurane is greatly restricted upon AChR binding. [^{14}C]Halothane photoincorporation shows no subunit preference, but the GA probe preferably photolabeled the M1-M3 transmembrane segments. Although the authors hypothesize a lipid-protein interface mode of interaction, electron paramagnetic resonance experiments demonstrated that isoflurane does not perturb the interaction of the headgroup of phospholipids with the AChR [46]. Thus, a more hydrophobic (closer to the lipid membrane core) or luminal localization of the GA site cannot be ruled out. Finally, photoincorporation of [^{14}C]halothane to rat cerebellar homogenates yielded multiple pholabeled proteins [47]. This is in accord with the existence of more than just one protein target accounting for the state of general anesthesia. More recently, [^{3}H]azietomidate was also synthesized and used for photoaffinity labeling of *Torpedo* AChRs [48]. The results indicated that [^{3}H]azietomidate photolabeled both α and δ subunits, preferably in the M2 transmembrane domain, more specifically at residues αGlu^{262} and δGln^{272} which are located in the extracellular mouth of the ion channel, as well as at residues δSer^{258} and δSer^{262} which are located in the cytoplasmic end of the ion channel. In addition, [^{3}H]azietomidate photolabeled several amino acids within the agonist binding site at both αγ and αδ subunit interfaces.

2. n-Alkanol Binding Sites

Although alkanols are not used clinically as GAs, they produce immobility, one of the main pharmacological properties elicited by GAs. Interestingly, their immobilizing potencies increase with increasing number of carbon atoms, but only up to a certain chain length (e.g., C12), after which n-alkanols with longer carbon chain decline in potency or remain equipotent with the preceding n-alkanol (reviewed in [2,49]). In this regard, the "cutoff" can be defined as the point at which the potency of the n-alkanol no longer increases with increasing carbon chain length. The existence of

Table 1. Binding Affinities of Inhalational Anesthetics for AChRs in Different Conformational States

Inhalational Anesthetic	Receptor Subtype	Conformation State			References
		Resting	Open	Desensitized	
		K_d, μM	IC_{50}, μM	K_i, μM	
Isoflurane	Human α4β2		82 [-70]		[62]
	Human α3β4		56 [-70]		[62]
	Human α2β4		25 [-70]		[62]
	Rat α4β2		34 ± 6 [-60]		[31]
	Rat α4β2		76 ± 4 [-70]		[43]
	Rat α4β2Val^{253}Phe		249 ± 5 [-70]		[43]
	Rat α4β2Val^{253}Trp		439 ± 18 [-70]		[43]
	Rat α4β2Val^{253}Tyr		1,906 ± 94 [-70]		[43]
	Chicken α4β2		11 [a] [-50]		[150]
	α7		700 ± 200 [-70]		[39]
	α7/5-HT$_3$R chimera		800 ± 200 [-70]		[39]
	Mouse α1β1γδ		1,160 ± 25 [-60]		[31]
	Mouse α1β1γδ		1,400 ± 100 [-50]		[29]
	Mouse α1Ser^{252}Ala/ β1Thr^{263}Alaγδ		300 ± 20 [-50]		[29]
	Mouse α1Ser^{248}Ala/ β1γδSer^{264}Ala		1,200 ± 100 [-50]		[29]
	BC$_3$H-1 cells		900 ± 100 [-50]		[29]
	Torpedo	360 ± 30			[45]
Halothane	Rat α2β4		47 ± 5 [-60]		[31]
	Rat α4β4		105 ± 17 [-60]		[31]
	Rat α4β2		27 ± 5 [-60]		[31]
	Rat α4β2		105 ± 7 [-70]		[37]
	Bovine α3β4		83 ± 4 [-60]		[38]
	Bovine α7		860 ± 60 [-60]		[38]
	Rat α7		552 ± 52 [-70]		[37]
	α7		1,200 ± 200 [-70]		[39]
	α7/5-HT$_3$R chimera		1,400 ± 400 [-70]		[39]
	Mouse α1β1γδ		870 ± 50 [-60]		[31]
	Torpedo Purified Native membrane	 180 ± 40 150 ± 40		 Similar to the resting state	[44]
	Torpedo			2.2 ± 0.3 %atm	[173]
Sevoflurane	Rat α4β2		98 ± 8 [-60]		[31]
	Mouse α1β1γδ		2,060 ± 110 [-60]		[31]
1-Chloro-1,2,2-trifluorocyclobutane	Human α4β2		330 [-70]		[62]
	Human α3β4		1,170 [-70]		[62]
	Human α2β4		440 [-70]		[62]

[a] This value corresponds to the K_i obtained from the competitive inhibition of ACh-induced ion channel openings.
Numbers between brackets are holding potentials in mV.

an alcohol cutoff has been hypothesized to reflect the molecular volume of the alcohol binding site on a putative ion channel target. Unique cutoff values for diverse nicotinic receptors may therefore reflect either differences in the size of the ion channel pore or nonluminal alcohol binding pockets.

2a. Long-chain n-alkanols

Long-chain n-alkanols (e.g., from n-pentanol to n-dodecanol) inhibit both muscle- [50,51] and neuronal-type AChR function [52,53] in a noncompetitive manner. Muscle-type AChRs can also be inhibited by n-propanol [51]. Other branched-chain alcohols (e.g., branched-chain pentanol analogs, 2-butene-1-ol, and 2-methyl-2-propanol) inhibit ACh-induced currents of the human α2β4 receptor as well [54]. In this regard, molecular volume cutoff values for the inhibition of α2β4 (n-decanol, 234 $Å^3$), α4β4 (≥ n-dodecanol; 276 $Å^3$) [52], α4β2 (n-decanol; 234 $Å^3$) [53], and *Torpedo* receptors (≥ n-decanol; 340 $Å^3$) [51,55] were determined. Depending on the concentration range, n-butanol either potentiated or inhibited ion channel function [53,54]. In addition to the length of n-alkanols, other structural factors such as hydrophobicity, shape, and flexibility are important for the potency and efficacy of alkanols on the AChR [54].

Identification of GA binding sites, including those for long-chain alcohols, using mutational studies is made all the more difficult because of the highly allosteric nature of AChR and homologous receptors. Discrete long-chain alcohol binding sites have been proposed to be either in the ion channel or at the lipid-protein interface of the AChR [56]. Studies indicating a luminal site location are (reviewed in [57], and references therein): **(1)** octanol inhibits preferentially the open state of the AChR; **(2)** mutations in either the segment M2-8/13 of the muscle-type α1 subunit or at position M2-13 of neuronal α4, β2, and β4 subunits influence the AChR sensitivity to long-chain n-alkanols. This is in accord with the evidence indicating that the octanol site does not overlap the QX-222 locus [26] which is between position M2-2 and M2-10 (see section III.2.a.); **(3)** mutations at Ser^{252} (position M2-10) alter hexanol sensitivity in parallel with the hydrophobicity of the side chain, suggesting a direct action between protein side chains and alcohol molecules; **(4)** unequal but additive effects of mutations on other AChR subunits, suggesting asymmetry in subunit interactions with alcohols; and **(5)** lack of effect of 1-hexanol in altering phospholipid headgroup interactions with the AChR [46].

In site-directed mutation studies the issue often becomes: do the amino acids identified as important for GA action contribute to a binding site or are they involved in transducing the effect of the GA? To circumvent this issue, a photoreactive alcohol, 3-azioctanol, was developed. 3-Azioctanol is an effective GA, producing a loss of righting reflex in tadpoles, potentiating $GABA_AR$ currents, and inhibiting mouse muscle-type AChR activation. Equally important, 3-[^{3}H]azioctanol is also an effective photoaffinity reagent, photoincorporating in the *Torpedo* AChR in a specific and conformationally-selective fashion [58]. The principal site of 3-[^{3}H]azioctanol photoincorporation in the *Torpedo* AChR was subsequently identified as Glu^{262} within the M2 segment of the α1 subunit. Therefore, the primary binding site for long-chain alcohols was established to be located in the outer or extracellular ring (position M2-20). Interestingly, the same binding location for the LA meproadifen was determined using meproadifen mustard as a photoaffinity labeling probe (see section III.2.a.). While identification of the 3-[^{3}H]azioctanol binding site in the mouth of the channel in the desensitized *Torpedo* AChR is an important milestone in GA research, this finding points immediately to at least one very important question: Is a long-chain alcohol binding site in the pore of LGIC receptors compatible with potentation of channel conductance in LGIC members such as the $GABA_AR$ and 5-HT_3R or must an unique binding site mediating this effect exist in these receptors? In the case of GlyR and $GABA_AR$, long-chain alcohol binding sites have been proposed to exist within cavities formed by the transmembrane segments of the subunits ([59]; reviewed in [2]). Nevertheless, the most direct answer to this question awaits future studies aimed at identifying the site of 3-[^{3}H]azioctanol photoincorporation in these receptors.

2b. Short-chain n-alkanols

Ethanol (in the millimolar concentratrion range) and other short-chain alcohols (e.g., methanol and propanol) enhance ACh-induced currents in muscle- [51,60] and neuronal-type AChRs [52-54,61,62]. This effect is opposite to the action of long-chain n-alkanols (see previous section). Ethanol effect is probably mediated by stabilization of the open ion channel [60] and/or by an increase in burst frequency [63]. Nevertheless, nonhalogenated alkane anesthetics such as cyclopropane and butane [64] as well as acetaldehyde, a primary metabolite of ethanol found in brain homogenates [65], failed to potentiate both AChRs and $GABA_ARs$.

Studying the effect of alkanols of similar molecular volume but with structural changes in the carbon backbone, Godden and Dunwiddie [54] hypothesized that alcohol molecules inducing potentiation of AChR ion channel function require certain structural flexibility. On the other hand, the α1Ser^{252}Ile mutation at position M2-10, which changes hydrophobicity but not size of the binding pocket, creates a sensitive inhibitory site for ethanol without changing the ethanol-induced gating modulation [60]. A mutation near the agonist binding site increased the potentiating effect of ethanol without affecting its inhibitory effect [60]. Interestingly, ethanol also induces inhibition of α7 [40,62] and α3β2 receptors [61]. The inhibition observed on α7 seems to be determined by the amino-terminal domain of the receptor [40].

These and the data from the previous section indicate that: **(1)** multiple binding sites for n-alkanols, at least an inhibitory and an enhancing site, may exist on the receptor. There are several reasons that support the existence of two allosterically-linked alcohol binding sites: ethanol does not compete sterically [43] but allosterically [53] with octanol for the inhibitory site, and the differential free energy change (for a review on thermodynamics of ligand-protein interactions see [20]) for the inhibitory effect is ~2-fold higher that that for the potentiation effect [53]; **(2)** depending on the receptor subtype the same alkanol may potentiate or inhibit the AChR; and thus **(3)**, there is not only one cutoff but a crossover from potentiation to inhibition [52].

3. The High-Affinity Barbiturate Binding Site

Barbiturates, in addition to inducing general anesthesia, exert a broad range of pharmacological actions including sedation and muscle relaxation, as well as anticonvulsant and anxiolytic effects [66]. Although the consensus view is that $GABA_A$Rs are the principal target for barbiturates (reviewed in [2,49,66]), there is also evidence that these drugs may inhibit neuronal-type AChRs and this may contribute to the pharmacological effect of barbiturates (reviewed in [43,67,68]). Barbiturate interaction with AChRs is also highly dependent on the conformational state of the receptor ([69,70]; reviewed in [2,71]). The cloning of multiple neuronal-type AChR subunits has precipitated an explosion of studies of barbiturate actions on recombinant receptors. Table **2** summarizes the concentration range for barbiturate binding to the resting, the open, and the desensitized state of AChRs from different origins.

Pharmacologically, barbiturates act as NCAs of AChR function (reviewed in [2,71,72]). Although thiopental competitively inhibits the human α7 receptor [73], it noncompetitively inhibits neuronal receptors from chromaffin [74] and PC12 cells [75]. Previous studies have also demonstrated the presence of a stereoselective, functional binding site on the AChR ([76,77]; reviewed in [2,71]). However, both α7 and α1β1γδ receptors do not show stereoselectivity to R(+) versus S(−) thiopental [73,77]. In addition, both convulsant [S(+)] and depressant [R(−)] enantiomers of 1-methyl-5-phenyl-5-propyl barbituric acid (MPPB) suppressed nicotine-induced currents in rat medial habenula neurons and PC12 cells with practically the same potency [67,78] (see Table **2**). These results suggest that there is no correlation between the noncompetitive inhibition of neuronal-type AChRs and the hypnotic or anticonvulsive effects of barbiturates *in vivo*.

The results of equilibrium binding experiments using *Torpedo* AChRs in the resting state demonstrate that amobarbital binds to a single high-affinity (K_d = 3.7 μM; see Table **1**) site [69]. Based on the mutually exclusive nature of barbiturate inhibition of 3-(trifluoromethyl)-3-(m-[^{125}I] iodophenyl]diazirine ([^{125}I]TID) photoincorporation and [^{3}H]tetracaine binding, this site is localized to the pore of the AChR ion channel [69]. From studies examining the inhibition of [^{125}I]TID photoincorporation into the receptor by different barbiturates, by positional isomers of amobarbital, and stereoisomers of pentobarbital and isobarbital, it is evident that two basic characteristics dominate barbiturate interaction with the resting channel: **(1)** a minimal level of barbiturate hydrophobicity and **(2)** steric hindrance. With respect to barbiturate hydrophobicity, shortening the 5' chain of amylbarbital or amobarbital by three carbons to produce barbital (5-ethyl, 5'-ethyl barbituric acid), reduces the hydrophobic character of the barbiturate molecule and results in a >500-fold reduction in potency for inhibition of [^{125}I]TID photoincorporation or [^{14}C]amobarbital binding ([69,70,79]) to the resting AChR. On the other hand, extending the length of the chain at the 5-position by an extra carbon (−CH_2−) converts pentobarbital to secobarbital, resulting in an increase in hydrophobicity as measured by the octanol/water partition coefficient but with no increase in potency for inhibition of [^{125}I]TID photoincorporation or [^{14}C]amobarbital binding [69,79]. In other words, high affinity binding to the AChR channel site requires that the barbiturate possesses a minimum level of hydrophobic character but once beyond that threshold level increased hydrophobicity does not appear to lead to increased binding affinity. The dramatic difference in inhibition potencies between the positional isomers of amobarbital clearly points out that steric constraints plays a significant role in barbiturate binding to the resting AChR channel. For example, by shifting the branch point on the 5' chain of amobarbital [5-ethyl, 5'-(3-methylbutyl) barbituric acid] by one carbon closer to the pyrimidine ring [i.e., isobarbital; 5-ethyl, 5'-(2-methylbutyl) barbituric acid] the result is a >10-fold reduction in the potency of inhibition of [^{14}C]amobarbital or [^{3}H]tetracaine binding, or [^{125}I]TID photoincorporation into the resting AChR [69,79]. The role of steric constraints in barbiturate binding to the resting AChR channel is further demonstrated by the approximately 2-fold differences in potency of inhibition between the R(+) and S(-) enantiomers of pentobarbital and isobarbital (see Table **2**).

Competition binding and photolabeling studies argue strongly that in the resting AChR the high-affinity barbiturate binding site overlaps that for tetracaine and TID [69]. The binding sites for TID and tetracaine in the resting AChR channel have been extensively characterized [80-82]. Tetracaine and TID bind to overlapping sites in the resting channel and for the smaller TID molecule that site is located between the highly conserved ring of leucine residues (M2-9; e.g., δLeu^{265}) and the more extracellular ring of valine residues (M2-13; e.g., δVal^{269}). TID is similar in size to pentobarbital (or amobarbital) and if we model pentobarbital complexed with the resting AChR channel [see Fig. **(3)**] we see that the barbiturate pyrimidine ring fits nicely in the TID binding site (defined by the segment between M2-9 and M2-13). If the barbiturate molecule is oriented such that the 5' chain extends downward towards the intracellular end of the channel, we see that the restriction in the lumen of the channel introduced by the leucine side-chains (M2-9) provides steric hindrance to barbiturate binding depending on the conformation of the 5' chain [Fig. **(3)**; cytoplasmic view]. We propose that the dramatic difference in inhibition potencies (i.e., binding affinity) between amobarbital and either pentobarbital or isobarbital, results from either the ability of the 5' chain of amobarbital (or amylbarbital) to adopt a more extended conformation compared to pentobarbital (or isobarbital) or from the reduced rotational freedom of the side chains of pentobarbital (or isobarbital). In either case the branching on the 5' chain of pentobarbital (or isobarbital) results in a bulkier conformation that provides steric hindrance to the binding of the barbiturate because of the narrow crevice, i.e., channel lumen (diameter ~7 Å), created by the ring of the leucine side chains (M2-9) (reviewed in [17]).

In the AChR resting state, we found that amobarbital was approximately 20-fold more potent than pentobarbital in inhibiting either [^{14}C]amobarbital or [^{3}H]tetracaine binding (see Table **2**), indicating a similar difference in binding affinity to the resting channel [69]. In contrast, the reported inhibition constants for the open channel conformation indicate a much smaller difference (1.4-fold) in potency between these two barbiturates [83]. Although the observed discrepancy may be caused by the difference in the origin of the used AChR, preliminary electrophysiological experiments

Table 2. Barbiturate Binding Affinities for AChRs in Different Conformational States

Barbiturate	Receptor Subtype	Conformation State			References
		Resting	Open	Desensitized	
		K_i (K_d), μM	IC_{50}, μM	K_i (K_d), μM	
Amobarbital	*Torpedo*	(12.0 ± 3.8)			[151]
	Torpedo	(3.7 ± 0.7)		(930 ± 380)	[69]
	Torpedo		82 ± 15 [0]		[70]
	Mouse muscle		30.0 ± 5.5 [-60]		[83]
Amylbarbital	*Torpedo*	3.3 ± 0.2		872 ± 35	[69]
Pentobarbital:					
Racemic	*Torpedo*	129 ± 8		338 ± 28	[69]
	BC_3H-1 cells		32 ± 2 [-50]		[76]
	Mouse muscle		42.0 ± 4.9 [-60]		[83]
	Torpedo		23 ± 4 [0]		[152]
R(+)	Torpedo	130 ± 15			[152]
	Torpedo	113 ± 5		233 ± 11	[69]
S(−)	*Torpedo*	201 ± 12		396 ± 15	[69]
	Torpedo	525 ± 46			[152]
Barbital	*Torpedo*	1,800			[69]
	BC_3H-1 cells		1,900 ± 200 [-50]		[76]
Secobarbital	Mouse muscle		100 ± 15 [-60]		[83]
	Torpedo		48 ± 8 [0]		[70]
	Torpedo	123 ± 15			[69]
Isobarbital:					
Racemic	*Torpedo*	144 ± 7		582 ± 28	[69]
R(+)	*Torpedo*	110 ± 24		320 ± 43	[69]
S(−)	*Torpedo*	209 ± 25			[69]
Thiopental	Rat medial habenula neurons		30.1 ± 7.5 [-60] (peak) 19.0 ± 3.3 [-60] (nondesensitized)		[67]
	PC12 cells		56.7 [-60] (peak) 7.4 [-60] (steady current)		[75]
	Chick α4β4		84 ± 22 [-60]		[105]
	Human α7		13 [a] [-60]		[73]
MPPB					
S(+)	PC12 cells		35.0 ± 3.2 [-60]		[78]
R(−)			41.0 ± 1.4 [-60]		[78]

Values between parentheses are K_ds.
Numbers between brackets are holding potentials in mV.
[a] This value is the K_i for the competitive inhibition of thiopental.

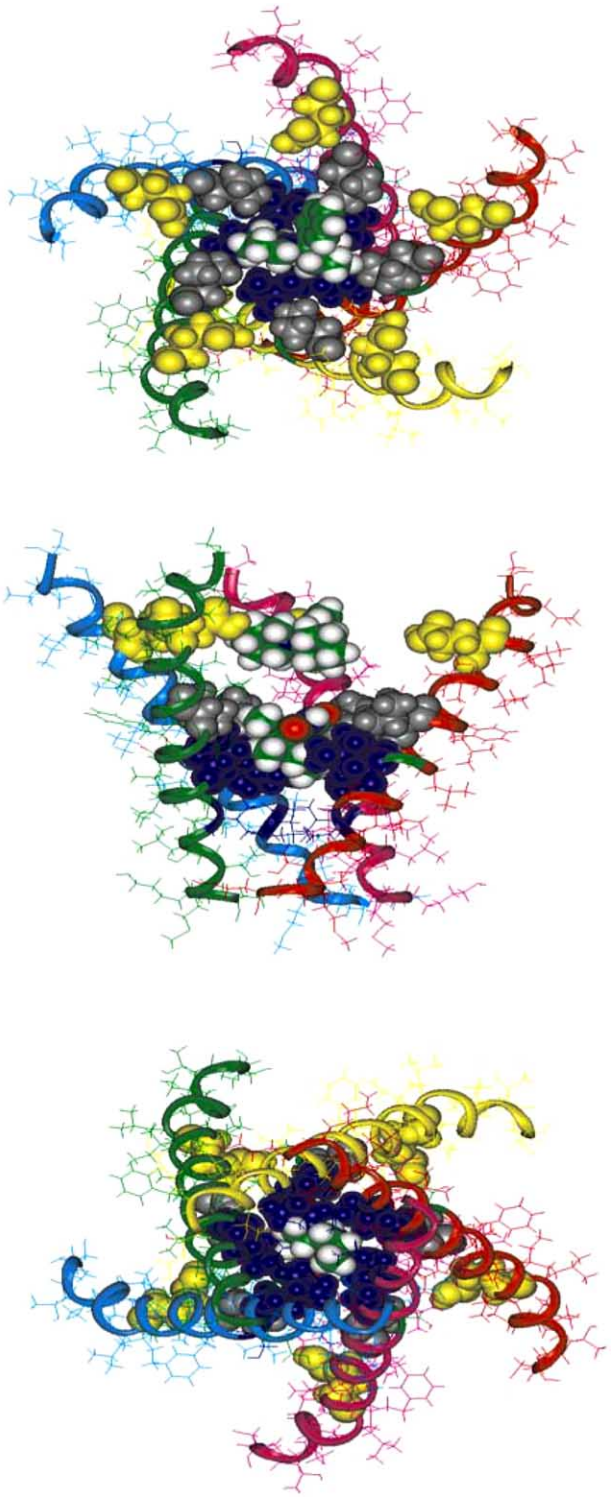

Fig. (2). Model of phencyclidine and pentobarbital binding sites in the resting AChR ion channel (modified from [71]). The amino acid sequence of the pore-lining α-helix of the homopentameric mechanosensitive receptor (1msl) was aligned with the sequence of M2 of

(Legend Fig. 2) contd…..

the α subunit from *Torpedo* AChR using the Clustal W program [114]. Then the aligned amino acid sequence from AChR was threaded onto the PDB coordinates of the backbone atoms of 1msl using the Homology module of Insight 2000. The resulting pentameric model of the pore-lining segment of AChR is shown viewed from the synaptic cleft (top), from the plane of the membrane (middle), and from the cytoplasmic side of the membrane (bottom). In order to better visualize phencyclidine and pentobarbital molecules (shown as space filling; CPK) within the pore, one M2 segment from the side view is not displayed. A molecule of phencyclidine is inserted above the valine ring (position M2-13; depicted in grey) close to the extracellular ring (position M2-20; depicted in yellow), according to [110,114]. A pentobarbital molecule is placed between the valine (position M2-13; depicted in grey) and the leucine ring (position M2-9; depicted in blue), according to [69]. The pyrimidine ring is positioned at about position M2-13, whereas the 1-methylbutyl group of the 5' chain of pentobarbital (the hydrophilic tail) provides steric hindrance to pentobarbital binding as a result of the restriction in the channel imposed by the side-chains of residues at position M2-9.

performed in *Torpedo* receptor-expressing cells suggest that there is only a ~5-fold difference in channel-inhibition potency between amobarbital and pentobarbital (reviewed in [71]). The affinities of amobarbital for the open channel of the *Torpedo* AChR is clearly similar to its affinity for the resting state, but both affinities are higher than that for the desensitized state [69]. On the contrary, pentobarbital exhibits a stronger preference for the open channel state than for either the resting or desensitized state [70,76]. There is very little information pertaining to the location of the barbiturate binding site in the open channel. One study [83], in which the triple mutation $Ser^{252}Ala$ (on both α1 subunits) and $Thr^{265}Ala$ (on the β1 subunit) decreased by 3.5-fold the dissociation rate constant of the local anesthetic QX-222 and by 3-fold the IC_{50} value for procaine, but resulted in no effect on amobarbital-induced inhibition, suggests that the barbiturate binding site is not located between position M2-6 and M2-10 in the open channel. In addition, site-directed mutagenesis studies suggest that although homologous amino acids $\beta 2Val^{253}$, $\beta 4Phe^{255}$, and $\alpha 4Val^{254}$ at position M2-13 determine the differential sensitivity to pentobarbital between the neuronal-type α4β2 and α4β4 receptor, it is unlikely that these residues form the barbiturate site proper [43].

4. Binding Sites for Dissociative Anesthetics

Although the N-methyl-D-aspartate receptor (NMDAR) and the AChR are not genetically related, they share certain pharmacological properties such as the noncompetitive inhibition elicited by a number of different dissociative anesthetics including PCP and its structural analogue thienylcyclohexylpiperidine (TCP), ketamine, and dizocilpine (reviewed in [2,19,20,49,71]). It is possible that these drugs have a similar mode of action on both AChR and NMDAR-type. Dissociative anesthetics are a special group of general anesthetics that provoke profound analgesia, amnesia, immobility, and hypnosis. As a pernicious side effect, they produce dysphoria, psychomotor activity, hallucinations, or delirium that limit their usefluness as clinical anesthetics.

4a. The High-Affinity Dizocilpine Binding Site

While dizocilipine is reported to be an open-channel blocker of α4β2 neuronal nicotinic AChRs [84], studies examining the mechanism of receptor inhibition [85] as well as the lack of stereoselectivity for its inhibition of α7 AChRs [86] suggest that dizocilpine inhibition may not simply result from steric blockade of open-channel AChRs. In this regard and to localize the dizocilpine binding site(s) on the muscle-type AChR, we used three different experimental strategies [87]. First, we determined the K_d and the number of binding sites of [^{3}H]dizocilpine when the receptor is in the desensitized or in the resting state. Secondly, we calculated the apparent K_i of dizocilpine from binding displacement experiments using NCAs that bind to different high-affinity sites on the AChR when it is in the desensitized or resting conformational state, respectively. Third, we partially resolved the structural components for dizocilpine action on the AChR by photoaffinity labeling and subsequent protease degradation and amino-terminal sequence analysis.

From the first set of experiments, we found that there is one (0.72 ± 0.05 binding site/AChR) high-affinity (K_d = 4.8 ± 1.0 μM) dizocilpine locus in the desensitized AChR, and several (3-6) low-affinity (140 μM) binding sites in the resting AChR (Table **3**). The high-affinity K_d value is in the same concentration range as that found for dizocilpine-induced inhibition of either agonist-induced ion channel opening [88] or of the potent NCA [^{3}H]histrionicotoxin ([^{3}H]HTX) binding in the desensitized state [89] (see Table **3**).

Taking into account the observed K_is for dizocilpine obtained from displacement of AChR-bound fluorescent NCAs such as quinacrine, ethidium, or crystal violet (CrV) from its respective high-affinity binding site on the AChR, we suggest that dizocilpine specifically inhibits the binding of quinacrine or CrV to desensitized AChRs or the binding of CrV to AChRs in the resting state [87]. Since ethidium binding is located within the ion channel [90,91], and ethidium binding is only inhibited by dizocilpine at very high concentrations, we conclude that the dizocilpine binding site is not located in the ion channel lumen. On the other hand, Schild-type analyses indicate that dizocilpine inhibition of CrV binding when the AChR is in the desensitized or resting conformational state is mediated by an allosteric mechanism [87]. Although there is presently no direct evidence for a luminal localization, indirect evidence (i.e., CrV specifically displaced the high-affinity NCA PCP) suggests a luminal ion channel localization of the CrV binding site [92]. Again, the experimental evidence suggests that the dizocilpine binding site is not located in the ion channel when the AChR is in either the desensitized or resting conformational state. 3,4,5-Trimethoxybenzoic acid 8-(diethylamino)octyl ester (TMB-8)-induced inhibition of [^{3}H]- or [^{125}I]-dizocilpine binding also supports this conclusion [87]. The fact that the n_H values obtained from these experiments were less than one (0.62 ± 0.05 and 0.50 ± 0.05, respectively) suggests that TMB-8 inhibits [^{3}H]dizocilpine binding by an allosteric mechanism. The pharmacological action of TMB-8 on muscle- and neuronal-type AChRs is believed to be mediated by ion flux inhibition upon binding to the ion channel [84,93,94].

Schild-type analyses also indicate that the inhibition of quinacrine binding is probably mediated by a steric mechanism. The fact that quinacrine-induced inhibition of [^{3}H]dizocilpine binding shows a n_H close to one also suggests a steric mode of inhibition. Considering that the high-affinity binding site for quinacrine (reviewed in [19,20]) is located apart from the ion channel [95], probably in a nonannular lipid domain of the desensitized AChR [96] 12 Å from the lipid-water interface [97], we may tentatively infer that the high-affinity dizocilpine binding site is located in a nonannular lipid domain close to the quinacrine locus. The exact location for the nonannular lipid domain on the AChR is unkown. However, indirect determinations have suggested that this domain may be located either between the five subunits of the AChR and/or between crevices existing within the four transmembrane segments (M1-M4) from each subunit (reviewed in [12,19,71]). Moreover, previous experiments indicated that quinacrine binding to desensitized AChR is sensitive to the action of fatty acids such as stearic acid and its 5-doxyl derivative [96,98]. Thus, further experiments were performed to test the hypothesis that dizocilpine binding site overalps the quinacrine locus. We observed that the maximal binding of [^{3}H]dizocilpine was not affected by stearic and arachidonic acid at concentrations higher than 1 mM (unpublished results). This suggests that in fact the dizocilpine binding site is close to the quinacrine locus but apart from the fatty acid domain.

In the third set of experiments we found that [^{125}I]dizocilpine photoincorporates into each AChR subunit, although principally into the α1 subunit. Within the α1 subunit the vast majority of [^{125}I]dizocilpine labeling maps to the transmembrane segment M1 and M4, demonstrating that dizocilpine binds at the lipid-protein interface of the receptor [99], a result consistent with the lipophilic nature of the dizocilpine molecule. However, several results indicate that some or all of the [^{125}I]dizocilpine labeling in the transmembrane segments M1 and M4 may not result from interaction with the high-affinity radioligand binding site on the receptor but with low-affinity sites at the lipid-protein interface. Dizocilpine binding to its high-affinity site on the desensitized state may result in only a very small component of specific photoincorporation that is masked by a much larger component of nonspecific labeling at the receptor lipid-protein interface. On the other hand, we demonstrated that there was no radioactivity associated with a fragment containing the M2 transmembrane segment of the α1 subunit, a result that argues against a luminal binding site for dizocilpine. However, our pharmacological experiments demonstrate that dizocilpine sterically competes for the quinacrine binding site when the AChR is in the desensitized state. In this regard, previous photolabeling experiments using quinacrine azide demonstrated that the quinacrine binding site is located in the M1 transmembrane segment of the α1 subunit at residues Arg^{209} and Pro^{211} [100]. In addition to these amino acids, site-directed mutagenesis experiments included the residue α1Tyr^{213} as another component of the quinacrine binding site [101]. In contrast, hydrophobic photolabeling studies implicate residue Pro^{211} in α1M1 as being situated at the lipid-protein interface [99]. Our results establish [^{125}I]dizocilpine photoincorporation into the α1M1 segment; therefore, one possibility is that residues within M1 contrib-

Table 3. Binding Affinities of Dissociative Anesthetics for AChRs in Different Conformational States

Dissociative Anesthetic	Receptor Subtype	Conformation State			References
		Resting	Open	Desensitized	
		K_i (K_d), μM	IC_{50} (K_d), μM	K_i (K_d), μM	
Dizocilpine	Torpedo	(140)		(4.8 ± 1.0)	[87]
	Torpedo	197 ± 25		5.8	[87]
	Torpedo	102 ± 12		13 ± 2	[89]
	Torpedo		3 [-70]; (7) [0]		[88]
	Human α4β2		18.7±3.4 [-100]; (7 ±50) [0]		[84]
	Human α2β2		36 [-70]		[68]
	Human α4β2		32 [-70]		[68]
	Human α3β2		20 [-70]		[68]
	Human α2β4		8.5 [-70]		[68]
	Human α4β4		4.5 [-70]		[68]
	Human α3β4		2.7 [-70]		[68]
PCP	*Torpedo*	(3.6 ± 0.8)		(0.80 ± 0.20)	[141]
	Torpedo			(0.46 ± 0.37)	[98]
	Torpedo	2.0		0.4	[153]
	Torpedo			(0.30 ± 0.10)	[151]
	Torpedo		1 [-60]		[149]
	Rat Muscle		20 [-60]		[149]
	Mouse muscle		31.3 ± 6.7 [-60]		[108]
	Electrophorus		(4 ± 1) [0]		[154]
	PC12 cells		0.7 [0]		[155]
TCP	*Torpedo*			(0.2)	[174]
	Torpedo			(0.25 ± 0.04)	[156]
	Torpedo	(0.83 ± 0.24)			[114]
Ketamine					
Racemic	*Torpedo*	16.5 ± 0.7		13.1 ± 1.8	[110]
	Torpedo	32 ± 3		17 ± 2	[157]
	Torpedo	42		6.6	[109]
	Mouse myotubes		2 (closed) [-30]		[158]
	PC12 cells		2.8 ± 0.6 [-60]		[175]
	Human α2β2		92 [-70]		[68]
	Human α4β2		72 [-70]		[68]
	Human α3β2		50 [-70]		[68]
	Human α2β4		29 [-70]		[68]
	Human α4β4		18 [-70]		[68]
	Human α3β4		9.5 [-70]		[68]
	Human α4β2		50 ± 4 [-60]		[159]
	Human α7		20 ± 2 [-60]		[159]
	Chick α4β4		0.24 ± 0.03 [-60]		[105]
S(+)	*Torpedo*	13.1 ± 1.8		15.4 ± 2.3	[110]
	PC12 cells		5.2 ± 0.5 (peak) [-60] 1.1 ± 0.2 (nondesensitized)		[115]
	SH-SY5Y cells		0.78 [-60]		[117]
R(−)	PC12 cells		5.4 ± 0.5 (peak) [-60] 1.7 ± 0.4 (nondesensitized)		[115]
	SH-SY5Y cells		3.58 [-60]		[117]

Values between parentheses are K_ds. Numbers between brackets are holding potentials in mV.

ute to both the lipid-protein interface of the AChR as well as to the high-affinity dizocilpine binding site.

Finally, the fact that dizocilpine binds the AChR closed channel with 5.3-fold higher affinity than for the open channel form is inconsistent with an open-channel-blocking mechanism [85,102], but supports our conclusion that the high-affinity dizocilpine binding site is located at a nonluminal site in the desensitized AChR. In this regard, our results are in agreement with an allosteric mode of inhibition for dizocilpine on the muscle-type AChR.

Certain neuronal-type AChRs might be involved in dizocilpine-induced anesthesia. Various neuronal-type AChRs are inhibited by dizocilpine at concentrations that depend on the receptor type ranging from 1 to 36 μM [68,84,86,89,103]. Table **3** summarizes the dizocilpine affinities for different AChR subunits. Specifically, receptors containing β4 subunits were more sensitive to dizocilpine than those containing β2 subunits, and α3-composed receptors were more sensitive than those containing the α2, α4, or α7 subunit [68,86].

4b. High-Affinity PCP/Ketamine Binding Sites

Dissociative anesthetics such as PCP [104] and ketamine [105] inhibit several neuronal-type AChRs at clinical concentration ranges. Thus, there exists the possibility that these compounds are in fact pharmacological determinants of dissociative anesthesia by affecting neuronal AChRs. One approach to understand how these compounds work is to determine the localization of its binding site(s). In this regard, photoaffinity labeling experiments using [^{3}H]azido-PCP have mapped the high-affinity PCP site on both the resting and desensitized AChR to a proteolytic fragment containing the transmembrane segments M1-M2-M3 [106]. In the muscle-type AChR open channel, the PCP binding site is believed to be located between the conserved ring of leucine residues (position M2-9) and the more cytoplasmic ring of serine residues (position M2-6) ([108]; reviewed in [19,71,107]) [see Fig. (**3**)]. This is consistent with the fact that PCP prevents photoincorporation of the high-affinity NCAs chlorpromazine (CPZ) to amino acids located at the threonine (position M2-2), serine (position M2-6), and leucine (position M2-9) ring [20]. However, a more complex process involving nonluminal inhibitory and regulatory sites for PCP has been hypothesized as well [108].

Ketamine competitively inhibits binding of both [^{3}H]PCP [109] and its analog [^{3}H]TCP [110] when the receptor is in the resting or desensitized conformation. Given the competitive nature of the interaction between ketamine and [^{3}H]TCP or [^{3}H]PCP for binding to the AChR and the structural similitude between ketamine, TCP, and PCP, it is likely that these dissociative anesthetics bind to a single or overlapping binding site. In order to characterize and potentially localize the binding site for the dissociative anesthetics ketamine and PCP in the resting AChR, we have taken into consideration previous studies that have established the binding sites for the well-known NCAs TID [80,82], tetracaine (see section III.2.b.), and barbiturates (see section II.3.) in the resting AChR channel. Our results yielded what appear to be conflicting conclusions: a mutually exclusive (competitive) interaction between ketamine/TCP/barbiturate/TID and tetracaine, but an allosteric interaction between ketamine/TCP/PCP and TID/barbiturate. More specifically:

(1) Ketamine, TCP [110], and PCP [111] increased the extent (i.e., potentiated) of [^{125}I]TID photoincoporation into AChR. Along these lines, previous photolabeling experiments have demonstrated that the effect of PCP is to subtly shift the orientation of the TID molecule within its resting channel binding site [112]. We conclude from these results that these dissociative anesthetics interact allosterically with TID, and that neither ketamine nor PCP (or TCP) binds between position M2-9 and M2-13, the established binding locus for TID within the resting AChR channel (see also [112]). Consistent with this conclusion, mutations at β2Val^{253} and α4Val^{254} (position M2-13) do not produce any effect on ketamine-induced inhibition of α4β2 neuronal-type AChR channels [68].

(2) Ketamine does not produce any effect on [^{14}C]amobarbital binding and the S(+) enantiomer of ketamine alone and TCP only slightly inhibit [^{14}C]amobarbital binding and with n_H values that deviate significantly from unity (n_H = 0.22-0.32). Reciprocally, amobarbital inhibits [^{3}H]TCP binding only marginally and again with a n_H value that is far from unity. These results are consistent with an allosteric interaction, if any, between S(+)ketamine/TCP and amobarbital, and that ketamine and TCP do not bind at the barbiturate binding locus within the resting AChR channel. Since the barbiturate binding site overlaps with that for TID [69], these results are in agreement with the previous conclusion.

(3) Ketamine, TCP [108] and PCP [113] completely inhibit [^{3}H]tetracaine binding to the resting AChR and the results strongly suggest a competitive, mutually exclusive interaction. In reciprocal fashion, our experiments indicate that tetracaine inhibits [^{3}H]TCP binding by a mutually exclusive (steric) mechanism, and that ketamine and TCP interact competitively. Collectively, the evidence demonstrates that these dissociative anesthetics bind to a single or overlapping sites on the resting AChR, and suggests that the ketamine/TCP/PCP binding site partially overlap the tetracaine site, which is located approximately between positions M2-16/17 and M2-5 [112] in the resting AChR channel.

These apparently conflicting conclusions can be reconciled by proposing the following: The extended conformation of the tetracaine molecule is longer than either the TID or barbiturate molecule [81], therefore there are at least two possibilities of how the ketamine (or PCP or TCP) molecule may be accommodated within the resting ion channel in order to partially overlap with the tetracaine binding site but allosterically interact with the TID/barbiturate locus. One possibility is that the ketamine (or PCP or TCP) binding site is located closer to the carboxyl terminal end of the M2 transmembrane segment (more extracellular, above M2-13 and closer to M2-20). Based on several lines of reasoning and the pattern of [^{3}H]tetracaine photoincorporation into M2-containing amino acids Gallagher and Cohen [81], positioned the tetracaine molecule within the resting AChR channel such that the dimethylaminoethyl group is in approximate register with M2-5 whereas its N-butyl group is aligned with hydrophobic residues toward the carboxyl-terminus of the M2 segment (e.g., M2-16/17). Because the

tetracaine molecule extends above M2-13, it therefore spatially overlaps the ketamine (or PCP or TCP) molecule, and this accounts for the competitive interaction between ketamine (or PCP or TCP) and tetracaine. In this regard, the model in Fig. (**3**) illustrates how PCP (or TCP or ketamine) and amobarbital (or TID) may bind simultaneously within the resting ion channel.

Newer structure-function relationship experiments using a series of adamantane derivatives to inhibit [^{3}H]TCP binding in both the resting and the desensitized state brought some light on the structure of the TCP binding site [114]. For instance, the results indicate that the TCP binding site in the resting state is very wide and that this locus does not impose any important structural restriction for binding except that the amino group on the adamantane derivative is necessary for full binding. On the contrary, a sharp correlation between molecular size or hydrophobicity versus K_i values was obtained in the desensitized state. This suggests that the TCP locus in the desensitized state is structurally different from the site in the resting state. One possibility is that the site for TCP in either state is located at different places within the ion channel: in the resting state, the TCP locus is located above position M2-13 and close to position M2-20, whereas in the desensitized state, this site is located between position M2-6 and M2-9 ([108,110,114]; reviewed in [19,71,107]). Thus, in order to construct a molecular modeling of the PCP binding site in the resting state [see Fig. (**3**)], the amino acid sequence of the pore-lining α-helix of the homopentameric mechanosensitive receptor (1msl) was aligned with the sequence of M2 of the *Torpedo* α1 subunit [114]. Then, the aligned amino acid sequence from AChR was threaded onto the PDB coordinates of the backbone atoms of 1msl. In this regard, Fig. (**3**) shows the binding domain of PCP in the resting state close to the mouth of the ion channel where a ring (extracellular or outer) of anionic residues is located at position M2-20. It is interesting to denote that the resting ion channel contains at least two allosterically-linked binding sites, one for PCP/TCP/ketamine and the other for TID/barbiturates.

Finally, it is noteworthy that ketamine inhibited [^{3}H]TCP binding to the resting and desensitized AChR in an apparently nonstereoselective manner [110]. This result is in agreement with the nonstereoselectivity inhibition of the open ion channel expressed in PC12 cells by ketamine isomers [115]. Supporting a nonstereoselective binding site for dissociative anesthetics is the fact that dexoxadrol and levoxadrol (PCP-like compounds) have no stereospecificity for inhibition of the nicotine-induced catecholamine secretion in adrenal chromaffin cells [116]. Nevertheless, these conclusions contrast with the fact that S(+)ketamine is nearly 4-fold more potent to inhibit ganglionic neuronal-type AChRs [117] (see Table **3**), 3-4 times better analgesic [118], 1.5-4 times better hypnotic [118,119], and 1.5-fold more potent in reducing ACh-induced neuronal excitation [120] than R(−)ketamine. The observed stereoselectivity argues in favor of the involvement of certain (but not all) neuronal-type AChRs in the anesthetic (or perhaps psychological and/or psychomotor) action of ketamine. The clinically-relevant concentration of ketamine in free plasma is 4-7 μM [121], and this concentration range is close to the IC_{50} values for certain neuronal-type AChRs (see Table **3**). Thus, this correlation also supports the above conclusion.

III. LOCAL ANESTHETICS

The inhibitory action of LAs on nerve conduction, the so-called local anesthesia, is primarily mediated by blocking voltage-gated Na^+ channels. Experimental evidence supports the conjecture that LAs may act on several voltage-gated and ligand-gated ion channels from the CNS as well. LA effects in the CNS include sedation, tremors, dysphoria, convulsions, and coma. Among LGICs, neuronal-type AChRs are possible targets for the action of LAs in the CNS.

1. Mechanism of Action

The early use of electrophysiological techniques such as voltage jump relaxation and agonist-induced noise spectra analysis demonstrated that LAs depress synaptic transmission by inhibiting the AChR (reviewed in [12,15]). These and subsequent studies on single-activated ion channels from both muscle- and neuronal-type AChRs supported the notion that the pharmacological action of LAs is elicited upon binding to the ion channel. Like other NCAs (reviewed in [19]), LAs exert their blocking action on AChRs reducing the duration of ion channel open time without changing maximal agonist binding. However, the mechanism of channel inhibition is still a matter of controversy. Experimental evidence supports the idea of channel blocking by a steric mechanism in which the drug enters into the lumen channel, binds and plugs it like a cork in a bottleneck. One of the earliest pieces of evidence supporting a steric mode of action was provided by voltage-clamp experiments where the inhibitory action of LAs, like other NCAs, was shown to be modulated by membrane potential changes (reviewed in [12,15]). Although almost all LAs are considered to be voltage-sensitive, uncharged LAs (e.g., benzocaine and dibucaine; [122]) and the unprotonated forms of all other LAs are voltage-insensitive because they cannot be expelled from the channel at positive potentials. In most cases, the inhibitory effect of quaternary LAs is more sensitive to membrane potential than the effect elicited by tertiary LAs. The potentiation of LA inhibition of transient agonist-evoked currents by membrane hyperpolarization can be quantified by calculating the e-fold change in the apparent IC_{50} value of the LA under study. In general, e-fold change values range from 26 mV for QX-222 in the neuronal α4β2 subtype [123] to 122 mV for procaine in parasympathetic neurons from rat intracardiac ganglia [124]. In addition, the observed values depend on both the LA and the AChR type. For instance, considering the same receptor class (e.g., rat α4β2 expressed in *Xenopus* oocytes), the e-fold change is 26 mV for QX-222 [121] or 90 mV for (-)cocaine [125]; whereas, considering the same LA (e.g., procaine) the values range from 50 [126] to 122 mV [124] for the muscle- and neuronal-type AChR, respectively. Taking into account the apparent voltage-sensitive location of LAs, the main conclusion is that LAs bind at a site within the electrical field, presumably the ion channel. More specifically, the binding site for QX-222 [123,124,127-130] and QX-314 [131] may be located closer to the cytoplasmic side of the receptor, whereas the procaine locus is near the middle of the ion channel [124,126,132], and the binding sites for (-)cocaine [133], bupivacaine [134,135] and piperocaine me-

thiodide [136] are much closer to the extracellular side of the receptor. Nevertheless, the QX-222 site location in the AChR ion channel from parasympathetic neurons [124] seems to be more external than in both $\alpha 1_2\beta 1\gamma\delta$ [127-130] and $\alpha 4\beta 2$ [123] subtypes.

On the basis of the experimental results described above and additional observations, the open-channel-blocking mechanism was postulated (reviewed in [12,15]). Although a great body of information supports the existence of an open-channel-blocking mechanism, deviations from this simple mechanism have been observed. For example, a cyclic model where the anesthetic binds to closed channels has also been suggested [126]. This evidence is in accord with the existence of an allosteric inhibitory mechanism. The interaction between the closed (e.g., resting, monoliganded, or biliganded) receptor and the ligand induces a conformational change on the protein preventing the opening of the ion channel and thus, depressing ion flux activity. An approach that allows us to distinguish between the two open-channel-blocking and allosteric mechanisms is determining the effect of LAs on both apparent channel opening and closing rate constants. If the open-channel-blocking is the main inhibitory mechanism, then, only the apparent rate constant for channel closing should decrease as LA concentration is increased. On the contrary, if the allosteric mechanism is the principal mechanism of inhibition, then, both apparent rate constants should decrease as the LA concentration increases. Utilizing fast kinetic techniques, Hess and coworkers, demonstrated that both apparent channel opening and closing rate constants decreased with increasing procaine concentrations, suggesting the existence of a regulatory site to which the LA binds before the channel opens [137]. The allosteric mechanism establishes that LAs bind to a regulatory site on the AChR, inhibit channel opening, and decrease the AChR in the open state by a slow course that converts to receptors in the active form. In other words, procaine preferably binds to the closed channel (A_nR) forming the A_nRL complex and thus, inhibiting ion flux ($A_nR'L$). In addition, tetracaine prefers the AChR in the resting state (R) forming the RL complex which reduces the conversion to the open channel (R'L). In the case of (-)cocaine, the rate of channel opening is not affected but the rate of channel closing is slightly (1.5-fold) increased [138]. The affinity of (-)cocaine for the open channel is 6-fold lower than that in the closed state (see Table **4**). Nevertheless, with the dissociative anesthetic dizocilpine (a drug that has been used as a palliative on cocaine addiction) the closing rate constant increases with increasing inhibitor concentration, whereas the opening rate constant does not change [102]. These results are consistent with a two step mechanism: first, (-)cocaine or dizocilpine rapidly binds to a regulatory site on the closed channel (A_nR) without affecting ion channel properties. In this regard, the ion channel might open with the drug bound (A_nR^*L). Next, the AChR-bound inhibitor complex (A_nRL) is slowly ($t_{1/2}$ 70 ms) transformed to a non-conducting state ($A_nR'L$). Alternatively, LAs may also bind to open channels with the subsequent inhibition of ion flux. In particular, the quaternary LA QX-222 binds preferably to the open channel (A_nR^*) forming the A_nR^*L complex and thus, inhibiting ion flux ($A_nR'L$). Probably, this latter mechanism is more important for quaternary than for tertiary LAs. Since the channel should be open before the LA inhibits it, the short time that the channel remains open will be enough for the initiation of the membrane depolarization process. Thus, the physiological implication of this mechanism is not obvious. The allosteric mechanism seems to be more significant for the inhibitory action of tertiary LAs. The existence of this regulatory mechanism may be of physiological relevance: the binding of an inhibitor to its regulatory site before the channel is open may ultimately preclude the signal transmission between cells. In turn, this perturbation of neurotransmission might be involved, at least partially, with the behavioral effects observed for (-)cocaine and their analogues including LAs. In this regard, the search for alternative drugs to alleviate the consequences of abusive use of cocaine and other derivatives should take into account a molecular structure that may compete for the cocaine site without producing its inhibitory effect.

2. High-Affinity Local Anesthetic Binding Sites

In addition to low-affinity LA binding sites at the lipid-protein interface ([139,140]; reviewed in [12,15]), there exist specific high-affinity LA binding sites which are displaced by other high-affinity NCAs. The evidence that high-affinity LAs present a stoichiometry of one binding site per functional AChR was determined by equilibrium binding of radiolabeled LAs such as meproadifen, trimethisoquin, tetracaine, as well as by 5-azido trimethisoquin photolabeling. Averaging all the experimental values, a stoichiometric ratio of 0.79 ± 0.37 LA binding site per AChR is calculated (reviewed in [12,15]). This ratio, which is close to unity, is similar to other high-affinity NCAs (reviewed in [19]).

LAs discriminate among different AChR conformational states: resting, open, and desensitized (reviewed in [12,15]). For instance, the decrease in the K_ds in the presence of agonists, is consistent with the preferential binding of LAs to the desensitized AChR. However, some LAs (e.g., procaine) do not have any preference with respect to the resting or the desensitized AChR, whereas others (e.g., tetracaine and piperocaine) prefer the AChR in the resting state. In addition, some quaternary LAs (e.g., QX-222) bind better the AChR in the open conformational state.

Interestingly, the affinity of LAs for muscle AChRs seems to be different to that from neuronal AChRs, and they also discriminate between distinct neuronal-type AChRs (Table **4**). In particular, procaine has a lower K_d for the receptor found in parasympathetic neurons [124] than that for other receptors. On the contrary, QX-222 binds the $\alpha 4\beta 2$ receptor with affinities one order of magnitude lower than other AChRs at the same voltage membrane (e.g., -90 mV; [123]). In addition, (-)cocaine has a lower IC_{50} value for the $\alpha 4\beta 4$ receptor than for other neuronal-type AChRs [125]. The observed differences in affinities (Table **4**) conjointly with the distinctions in voltage sensitivity existent among LAs on several AChRs might help to identify the structural components involved in the LA binding site.

One of the most important techniques used to discern the localization of high-affinity LA binding sites is the photoaffinity labeling approach. This can be achieved using radiolabeled LAs that can be directly activated by UV light, or using other photoactivatable derivatives with specific photore-

Table 4. Local Anesthetic Preference for the in the Different Conformational States of the AChR.

Local Anesthetic	Conformational State				References
	Resting **K_d, μM**	**Desensitized K_d, μM**	**Open IC_{50}, μM**	**Membrane voltage, mV**	
Procaine	790 ± 80 (*T. ocellata*)	690 ± 120 (*T. ocellata*)		0	[160]
			88 ± 10 ($\alpha 1_2\beta 1\gamma\delta$; BC_3H-1) 110 ± 50 (rate constant for channel closing) 40 ± 60 (rate constant for channel opening)	-60 -60 -60	[137]
			15 ± 2 ($\alpha 1_2\beta 1\gamma\delta$; Mouse) 50 ± 9 ($\alpha 1_2\beta 1\gamma\delta$; Mouse)	-90 -45	[83]
			100 ($\alpha 1_2\beta 1\gamma\delta$; Mouse)	-40	[161]
			70 ($\alpha 1_2\beta 1\gamma\delta$; Mouse)	-80/-90	[162]
			35 (CCh-evoked catecholamine secretion) 80 ($^{22}Na^+$ influx in chromaffin cells)	0 0	[163]
			100 ($^{22}Na^+$ influx in PC-12 cells)	0	[155]
			2.8 (Parasympathetic neurons)	-80	[124]
			40 ± 3 ($^{86}Rb^+$ influx in *T. californica* vesicles)	-25	[154]
Tetracaine	0.5 ± 0.1 (*T. californica*)	29 ± 7 (*T. californica*)		0	[113]
			1 ($\alpha 1_2\beta 1\gamma\delta$; electrocyte) 38 ($\alpha 1_2\beta 1\gamma\delta$; BC_3H-1)	-60 -80	[149]
	0.31 ± 0.03 (*T. californica*)			0	[110]
(-)Cocaine	50 ± 10 (BC_3H-1)		300 ± 70 (BC_3H-1)	-90	[138]
			6-14 (Cs^+ influx in *E. electricus* vesicles) 58 (Cs^+ influx in *T. californica* vesicles)	0 0	[154]
			10 ($^{22}Na^+$ influx in PC-12 cells)	0	[155]
			17 (Frog sartorius muscle)	-100	[133]
			4.4-6.9 ($\alpha 4\beta 2$; Rat) 22.0-42.3 ($\alpha 3\beta 2$; Rat)	-70 -70	[164]
			2 ($\alpha 4\beta 4$; Rat)	-50	[125]
			6 ± 1 ($\alpha 3\beta 4$; Rat)	-50	[125]
			16 ± 4 ($\alpha 2\beta 4$; Rat)	-50	[125]
			15 ± 1 ($\alpha 4\beta 2$; Rat)	-50	[125]
			41 ± 9 ($\alpha 2\beta 2$; Rat)	-50	[125]
			60 ± 18 ($\alpha 3\beta 2$; Rat)	-50	[125]
			0.81 (nicotine-elicited hippocampal noradrenaline release; Rat)	0	[165]
Lidocaine	>1000 (*T. occelata*)	150 ± 10 (*T. occelata*)		0	[160]

(Table 4) contd…..

Local Anesthetic	Conformational State				References
	Resting **K_d, μM**	**Desensitized K_d, μM**	**Open IC_{50}, μM**	**Membrane voltage, mV**	
Piperocaine	0.33±0.08 (*T. occelata*)	4.2 ± 1.1 (*T. occelata*)		0	[160]
	0.8 (*T. californica*)	55 (*T. californica*)		0	[113]
Benzocaine			114 ± 48 (*Rana temporaria* muscle)	-70	[166]
	500 ± 50 (*D. tschudii*)			0	[96]
Dibucaine	3.0 (*T. californica*)	0.24 (*T. californica*)		0	[167]
Bupivacaine	25 ± 5 (*T. californica*)	3 ± 1 (*T. californica*)		0	[135]
Bupivacaine Methiodide	3.2 ± 0.4 ($\alpha 1_2\beta 1\varepsilon\delta$; Rat)	0.75 ± 0.08 ($\alpha 1_2\beta 1\varepsilon\delta$; Rat)		0	[135]
QX-222			29 (Frog muscle)	-120	[127]
			28 (Parasympathetic neurons)	-80	[124]
			20 (Rat myoballs)	-120	[168]
			141 ($\alpha 4\beta 2$; Mouse) 18 ($\alpha 1_2\beta 1\gamma\delta$; BC_3H-1)	-150 -150	[123]
			76.5 ± 7.8 ($\alpha 1_2\beta 1\gamma\delta$; Mouse) 20.0 ± 0.9 ($\alpha 1_2\beta 1\gamma\delta$; Mouse)	-110 -150	[129]
			9 (*Rana pipiens* muscle)	-80	[169]
QX-314			1 (Frog muscle)	-100	[127]
C6SL-MeI	20 (*T. californica*)	0.87 (*T. californica*)		0	[170]
Proadifen	7 (*T. californica*)	0.6 (*T. californica*)		0	[171]
Meproadifen	6.2 ± 3.0 (*T. marmorata*)	0.5 ± 0.2 (*T. marmorata*)		0	[141]
	25 (*T. californica*)	0.3 (*T. californica*)		0	[171]
Adiphenine	5 ± 2 (*T. californica*)	7 (*T. californica*)		0	[172]
Dimethisoquin	5.0 (*T. californica*)	1.1 (*T. californica*)		0	[167]
Trimethisoquin	3.2 ± 0.9 (*T. marmorata*)	1.2 ± 0.3 (*T. marmorata*)		0	[141]

active groups. The specificity of the photoaffinity labeling experiments followed the criteria: **(a)** existence of a positive displacement elicited by other known high-affinity NCAs, **(b)** enhancement of affinity and thus labeling of the LA under study (but not for all) in the presence of agonists, and **(c)** inhibition of the agonist effect by competitive antagonists such as α-bungarotoxin (α-BTx).

One of the first labeling experiments to localize the LA binding site was performed using different azido LA derivatives (reviewed in [12,15]). The azido-procainamide deriva-

tive only labeled the AChR α1 subunit, whereas the 5-azido[^{3}H]trimethisoquin derivative labeled the δ subunit in a HTX- and CCh-sensitive fashion. The same basic pattern was observed using [^{3}H]trimethisoquin and simple UV irradiation [141,142]. Similar results were observed using other tritiated NCAs (reviewed in [19]). The LA analog meproadifen mustard, as well as other NCAs, also labeled the α1 and γ subunit [143].

2a. Binding Sites for Quaternary Local Anesthetics

The outer or extracellular ring is the labeling site for the potent LA derivative meproadifen mustard. Meproadifen mustard was initially found in a fragment beginning at Ser^{173} of the α1 subunit. More precisely, the meproadifen derivative labeled the α1 subunit at position Glu^{262} [143]. Based on the four transmembrane AChR structural model [see Fig. **(1)**], there is consensus that this ring of negative charges is located between the synaptic membrane and the extracellular domain of the AChR (the M2-M3 loop, closer to M2), probably at or near the internal mouth of the channel [Fig. **(3)**]. Interestingly, these results indicate that the LA meproadifen (and probably its tertiary analog proadifen) shares the same binding locus as GA alcohols (see section II.2.a.).

The side chains of photolabeled amino acids such as α1Ser^{248} for the neuroleptic CPZ and α1Glu^{262} for the LA meproadifen should be approximately 15 Å apart each other. This fact provides support for the extension of the early hypothesis of only one locus for structurally-unrelated high-affinity NCAs to the existence of several binding sites for different NCAs all located into the channel lumen (reviewed in [12,19]).

Meproadifen, as well as other LAs, shifts the equilibrium to the desensitized state (see Table **4**). This was evidenced when the labeling of α1Tyr^{93}, an amino acid involved in the agonist/competitive antagonist binding site at the α1 subunit (reviewed in [1]), elicited by the irreversible antagonist *p*-N,N-(dimethylaminoi)phenyldiazonium fluoroborate was augmented in the presence of meproadifen. This experimental evidence suggests that this residue is more accessible to labeling when the AChR is in the desensitized state.

The localization of the QX-222 binding site was proposed on the basis of site-directed mutagenesis and patch-clamp studies ([129]; reviewed in [12,15]). For instance, the pharmacological activity of the open-channel blocker QX-222 is affected when the serine ring (position 6) is mutated. The drug presented shorter time in the AChR-bound state and its K_d was augmented when the polar amino acid α1Ser^{248} was mutated to Ala, a nonpolar amino acid. In comparison, the δSer^{262}Ala mutation also affected these properties but in an extent two times lower than the one detected in the α1 subunit. This effect can be interpreted in the light of difference in the number of residues mutated (there are two α1 subunits per each δ). A double mutation (actually a triple mutation) produced an additive effect on the K_d of QX-222. However, the observed lifetime (1.5 ms) for QX-222 in the wild type AChR is similar (1.2 ms) to that obtained in the double mutated [129]. Additional mutations on position 2 produce a similar pattern as that observed by mutations on position 6, however, the effect on the QX-222 K_d was small. In contrast with the experimental evidence on serine ring mutations, when α1Ser^{252} (position 10, located one residue apart from the leucine ring) was mutated to Ala, both the affinity of QX-222 and the lifetime of the AChR-QX-222 complex were enhanced. The increased affinity was principally due to a decrease in the dissociation rate constant values and it was not affected by voltage membrane changes [129]. Mutations β1Phe^{259}Ser and α1Ser^{252}Ala on the $\alpha1_2\beta1\delta_2$ (γ-less) receptor showed similar relative effect of QX-222 blockade as in the $\alpha1_2\beta1\gamma\delta$ receptor [128]. The Thr^{264}Pro mutation in the ε subunit, which has been implicated as responsible of one of the congenital myasthenic syndromes (reviewed in [12,15]), only slightly affects the inhibitory property of QX-222 [144]. Thus, Thr^{264}, which is located close to the valine ring, may not be involved in the QX-222 binding site. In addition, QX-222 produced the same effect on both adult ($\alpha1_2\beta1\varepsilon\delta$) and embryonic ($\alpha1_2\beta1\gamma\delta$) muscle-type AChRs (see Table **4**). Considering that the structural determinants that account for the functional differences between both channels are located at the M3-M4 loop, the M4 segment, and the extracellular portion of both channels, the QX-222 locus should be positioned neither in the extracellular nor cytoplasmic hydrophilic portions nor in the M4 transmembrane fragment but, as was previously addressed, within the ion channel.

Concerning neuronal AChRs, QX-222 has been shown to block the AChR in rat parasympathetic ganglion cells, in the clonal cell line PC12, in the α7 subtype, and in the α4β2 neuronal receptor (see Table **4**). Notably, the α4β2 receptor type showed a much lower sensitivity to QX-222 than other AChRs. The structural components that confer this affinity distinction might be elucidated by considering which amino acids on the M2 domain of the AChR types are different. In chick brain α7 receptors, the pharmacological effect of QX-222 was abolished by mutation of the leucine ring, in particular Leu^{247} to polar residues such as Thr or Ser [145]. As expected, mutations on amino acids related to the agonist binding site on the α7 AChR, did not significantly change the pharmacological properties of QX-222 (reviewed in [12,15]).

Based on these results, it is conceivable that the quaternary ammonium group of QX-222 is positioned close to Ser^{248}, which is part of the conserved serine ring (position 6). Taking into account that the secondary structure of the M2 transmembrane domain of the α1 subunit is α-helical, Ser^{248} would be positioned one turn away from Ser^{252}. In turn, α1Ser^{252} (position 10) is located one residue apart from the leucine ring (position 9). Thus, the aromatic moiety of the QX-222 molecule is near the leucine ring, 5.7 Å away from the serine ring (reviewed in [12,15]).

The blocking rate of QX-314 is similar to that of its triethylamine structural analog QX-222. However, QX-314 remains in the ion channel for longer time (an order of magnitude more) than QX-222 does. Thus, QX-222 is termed a fast channel blocker whereas QX-314 is called a slow channel blocker. Nevertheless, testing the protection elicited by QX-314 on the reaction of methanethiosulfonate derivatives with several Cys-substituted (one at a time) residues in the M2 segment of the mouse α1 subunit, Pascual and Karlin [146] considered that both LAs practically share the same locus. When the channel was open, QX-314 protects com-

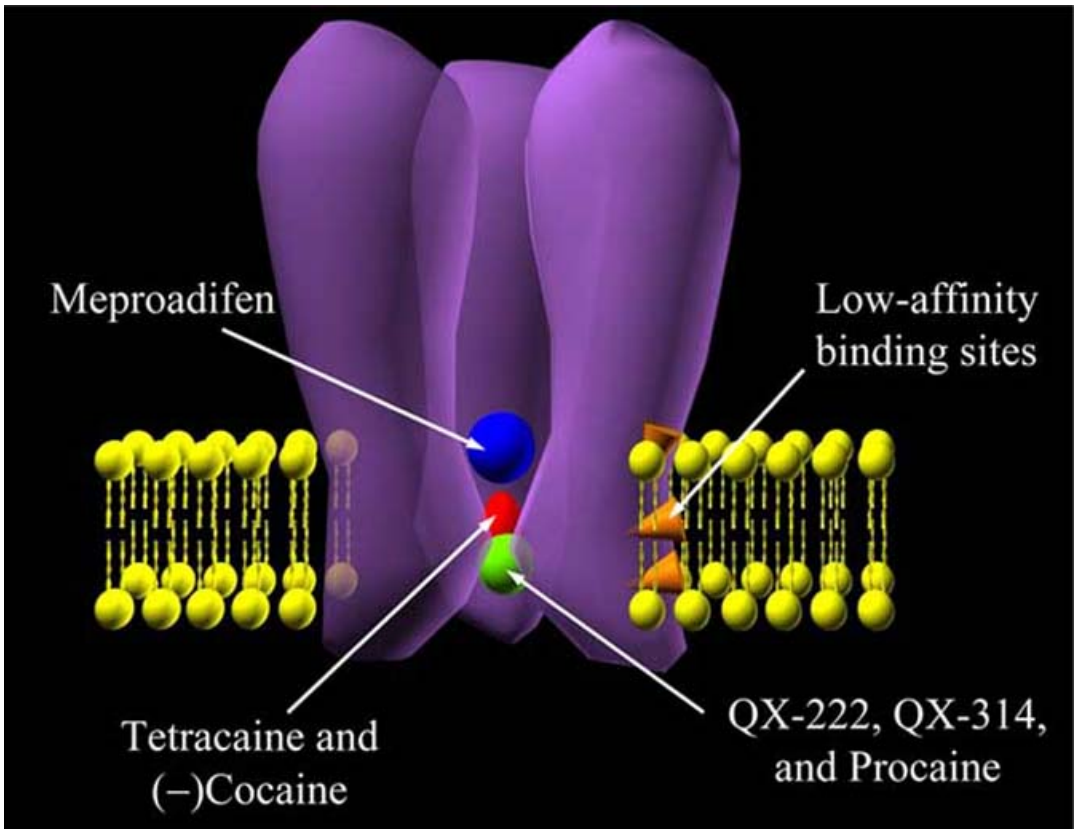

Fig. (3). Transverse schematic view of the AChR (only three subunits are shown for simplicity) showing the most probable localization for several LA binding sites (modified from [15]). The photolabeling site for meproadifen mustard (blue) is located at the extracellular or outer ring of the desensitized AChR. Additional photoaffinity labeling studies indicate that the binding site for tetracaine (red) is located between the serine and the valine ring (including the leucine ring) of the resting AChR. Mutagenesis experiments and accessibility studies indicate that the locus for QX-222 and QX-314 as well as for procaine (green) is positioned at both the serine and the leucine ring in the open ion channel conformation. Additional mutagenesis studies in the open state suggest that the (-)cocaine binding site (red) is located at the valine ring and perhaps at the serine ring. The orange cones indicate the possible location for low-affinity LA binding sites at the lipid-protein interface.

pletely the Cys mutants on the α1 subunit located at Glu^{241}, Thr^{244}, and Ser^{248}, and moderately those located at Leu^{251} and Val^{255}, whereas both Leu^{258} and Glu^{262} to Cys mutants were not protected by the drug. This evidence suggests that QX-314 binds to the open ion channel and that its locus is found at residues located between Glu^{241} and Leu^{251} of the α1M2 domain. The portion of the channel containing the sequence between Gly^{240} and Thr^{244} is close to the cytoplasmic side of the ion channel and it is suggested to be involved in the activation gate [147]. In addition, no protection was observed when the channel was in the resting [146] or in the desensitized [148] state. Another possibility is that QX-314 binds to the same site as QX-222 [see Fig. (**3**)] at the portion between $\alpha1Ser^{248}$ and $\alpha1Ser^{252}$, and thus, the passage of the methanethiosulfonate reagent to the Cys-substituted residues located in a more constricted region of the ion channel, namely the gate, is consequently inhibited.

2b. Binding Sites for Tertiary Local Anesthetics

Previous experiments demonstrate that specific labeling of the NCA [^{125}I]TID of the AChR is inhibited by tetracaine and dibucaine in the presence of α-BTx (reviewed in [12,15]). This is in accord with the fact that tetracaine binds preferentially the AChR in the resting state (see Table **4**). Thus, tetracaine might be competing with [^{125}I]TID labeling by a mutually exclusive mechanism. Since the TID binding site has been found to be located at the valine and leucine rings (reviewed in [19]), the tetracaine locus should be close to these rings. In fact, photoaffinity labeling studies using [^{3}H]tetracaine under UV activation indicate that this LA incorporates with similar efficiency to α1, β1, γ, and δ subunits [113]. More specifically, [^{3}H]tetracaine labeled two sets of homologous hydrophobic residues: one comprised by $\alpha1Leu^{251}$, $\beta1Leu^{257}$, γLeu^{260}, and δLeu^{265} [leucine ring (position 9)] and another formed by $\alpha1Val^{255}$ and δVal^{269} [valine ring (position 13)] as well as residues δAla^{268} (position 12) and $\alpha1Ile^{247}$ (position 5) [81]. The residues from both subunits are almost coincident with the TID-labeled amino acids in the resting state as well as with the CPZ-labeled amino acids in the desensitized state (valine and leucine rings). In this regard, a model for the tetracaine binding site was suggested [81]: the benzene ring (6.5 Å) is positioned at the leucine ring (position 9) with its *N*-butyl chain (4 Å wide in extended configuration) interacting with hydropho-

bic residues from both position 12 and 13 (valine ring), and the dimethylamino group (probably protonated) interacting with hydrophilic residues located close to the serine ring (position 6). The possibility of interaction between the butylamino group of tetracaine and hydrophobic residues from position 12 and 13 is supported by the fact that procaine, which lacks the butyl group on the *N*-aryl moiety, interacts with the resting AChR with 1,000-fold lower affinity than tetracaine [113] (see Table **4**). In addition, the fact that tetracaine is 10 times more potent as an inhibitor of *Torpedo* than of mouse muscle AChRs can be explained by natural substitutions found in each receptor [149]. In this regard, one of the four natural substitutions (Ser to Phe at position 6 from the β1 subunit) decreases the polarity at position 6 (serine ring) reducing the favorability of interaction with the charged dimethylamino group of tetracaine. Additional residues labeled by [^{3}H]tetracaine (δAla^{268} and α1Ile^{247}) extend the definition of the surface of the M2 helix that is oriented toward the channel lumen in the resting (closed) state beyond those side chains labeled by [^{125}I]TID (residues 9 and 13; reviewed in [19]).

The location of the procaine binding site has also been studied by site-directed mutagenesis [83]. The inhibitory effect of procaine on dimethylphenylpiperazinium-evoked ion channel activity of the mouse muscle AChR was increased when the double mutant α1Ser^{252}Ala/β1Thr^{265}Ala was used (see Table **5**). Based on this evidence, a procaine binding site location similar to that determined for QX-222 (see previous section) is assumed. Interestingly, the same mutations did not affect the inhibitory properties of barbiturates. These results indicate that in the open channel confor-

Table 5. Residue Mutations on the M2 Transmembrane Domain of Different AChRs Affecting Local Anesthetic Affinity

Local Anesthetic	Mutation Mutation	Source of AChR	Pharmacological effect (fold)		References
			Affinity Increase	Affinity Decrease	
QX-222	α1Ser^{252}Ala	Mouse α1$_2$β1γδ	1.9	–	[129]
	β1Thr^{263}Ala		1.8	–	
	α1Ser^{252}Ala/β1Thr^{265}Ala		3.4	–	
	α1Ser^{248}Ala		–	2.0	
	β1Phe^{259}Ser		1.7	–	
	δSer^{262}Ala		–	1.3	
	α1Ser^{248}Ala/δSer^{262}Ala		–	2.7	
	α1Thr^{244}Ala		1.2	–	
	β1Gly^{255}Ser		1.3	–	
	γThr^{253}Ala		1.3	–	
	δSer^{258}Ala		–	1.1	
	α1Thr^{244}Ala/β1Gly^{255}Ser		–	1.3	
	γThr^{253}Ala/δSer^{258}Ala		–	1.5	
	α1Ser^{252}Ala	Mouse α1$_2$β1δ$_2$ (γ-less)	1.4	–	[123]
	β1Phe^{259}Ser		1.3	–	
	εThr^{264}Pro	Mouse α1$_2$β1εδ	1.5	–	[143]
	α7Leu^{247}Thr (or Ser)	Chick α7	–	Abolished	[145]
	α7Leu^{247}Phe		–	1.5	
	α7Leu^{247}Val		–	1.1	
Procaine	α1Ser^{252}Ala/β1Thr^{265}Ala	Mouse α1$_2$β1γδ	3.0	–	[83]
(-)Cocaine	β4Phe^{255}Val	Rat α3β4	–	8.3	[125]
	β2Val^{253}Phe	Rat α3β2	3.5	–	

mation, the binding site for procaine is distinct to that for barbiturates. In this regard, a general conclusion might be stated: only certain GAs bind to the same locus as some LAs. However, it is neccesary to take into consideration that the results from our laboratory (competitive binding of tetracaine and barbiturates, ketamine, or PCP; [110,114]) were done with *Torpedo* AChRs in the resting state whereas the experiments showing differential sensitivity between procaine and barbiturates to M2 mutated-containing receptors were performed in oocyte-expressing mouse AChRs in the open conformational state [83].

Regarding the localization of the cocaine binding site, recent experimental evidence using several neuronal AChR subtypes, chimeras, and mutants, has suggested that β4Phe^{255} [valine ring (position 13)] of the α3β4 receptor subtype (see Table **4**) is structurally involved with the high-affinity (-) cocaine locus [125]. There are two possible modes of interactions: (a) one possibility is that the protonated amine group of cocaine interacts with the aromatic ring of Phe by cation-π interactions. In this case, the voltage-dependence of (-) cocaine inhibition might arise from the electrostatic nature of the cation-π interaction. The other possibility (b) is that the cocaine phenyl ring is interacting with the aromatic moiety of Phe. In this case, and considering that cocaine has a size of about 12 x 6 Å, the amine group might project deeper into the ion channel to reach position 6 (serine ring). Additional evidence suggests that (-)cocaine may allosterically inhibit the α4β2 receptor subtype by binding to a nonconserved stretch of 50 amino acids preceding the M1 domain [125].

ACKNOWLEDGEMENTS

This review was supported by Western University Health Sciences Intramural Grants (to HRA) and by the Master in Sciences Program, Department of Pharmaceutical Sciences (to PB).

ABBREVIATIONS

GA	=	General anesthetic
LA	=	Local anesthetic
AChR	=	Nicotinic acetylcholine receptor
NCA	=	Noncompetitive antagonist
LGIC	=	Ligand-gated ion channel
5-HT$_3$R	=	Type 3 5-hydroxytryptamine (serotonin) receptor
GlyR	=	Glycine receptor
GABA$_A$R	=	γ-Aminobutyric acid receptor
K_d	=	Dissociation constant
IC_{50}	=	Competitor concentration that inhibits 50% drug maximal binding
EC_{50}	=	Drug concentration that induces 50% receptor activity
[^{125}I]TID	=	3-(Trifluoromethyl)-3-(m-[^{125}I]iodophenyl)diazirine
PCP	=	Phencyclidine [1-(1-phenylcyclohexyl)piperidine]
TCP	=	1-(2-Thienylcyclohexyl)piperidine
HTX	=	Histrionicotoxin
[^{3}H]HTX	=	[^{3}H]histrionicotoxin
n_H	=	Hill coefficient
CrV	=	Crystal violet
CPZ	=	Chlorpromazine
α-BTx	=	α-Bungarotoxin
TMB-8	=	3,4,5-Trimethoxybenzoic acid 8-(diethylamino)octyl ester
CNS	=	Central nervous system
NMR	=	Nuclear magnetic resonance
AChBP	=	Acetylcholine binding protein
MPPB	=	1-Methyl-5-phenyl-5-propyl barbituric acid.

REFERENCES

[1] Arias, H.R. **(2000)** *Neurochem. Int*., *36*, 595-645.
[2] Arias, H.R., Machu, T.K., Trudell, J.R. and Blanton, M.P. **(2002)** in *Recent Research Developments in Biophysical Chemistry* (Condat, C.A. and Baruzzi, A., Eds.), pp. 123-154. Transworld Research Network / Research Signpost, India.
[3] Ortells, M.O. and Lunt, G.G. **(1995)** *Trends Neurosci., 18*, 121-127.
[4] Brejc, K., van Dijk, W.J., Klaassen, R.V., Schuurmans, M., van der Oost, J., Smit, A.B. and Sixma, T.S. **(2001)** *Nature, 411*, 269-276.
[5] Sine, S.M. **(2002)** *J. Neurobiol*., *53*, 431-446.
[6] Chou, K. C. **(2004)** *Biochem. Biophys. Res. Commun., 319*, 433-438.
[7] Chou, K. C. **(2004)** *Biochem. Biophys. Res. Commun., 316*, 636-642.
[8] Keramidas, A., Moorhouse, A.J., Schofield, P.R. and Barry, P.H. **(2004)** *Prog. Biophys. Mol. Biol*., *86*, 161-204.
[9] Swope, S.L., Moss, S.J., Raymond, L.A. and Huganir, R.L. **(1999)** *Adv. Second Messenger Phosphoprot. Res*., *33*, 49-78.
[10] Millar, N.S. **(2003)** *Biochem. Soc. Trans*., *31*, 869-874.
[11] Anand, R., Conroy, W.G., Schoepfer, R., Whiting, P. and Lindstrom, J. **(1991)** *J. Biol. Chem*., *266*, 11192-11198.
[12] Arias, H.R. **(1999)** *Neurosci. Biobehav. Rev*., *23*, 817-843.
[13] Palma, E., Bertrand, S., Binzoni, T. and Bertrand, D. **(1996)** *J. Physiol*., *491*, 151-161.
[14] Lloyd, G.K. and Williams, M. **(2000)** *Pharmacol Exp Ther*., *292*, 461-7.
[15] Arias, H.R. and Blanton, M.P. **(2002)** *Mini. Rev. Med. Chem*. *2*, 385-410.
[16] Tassonyi, E., Charpantier, E., Muller, D., Dumont, L. and Bertrand, D. **(2002)** *Brain Res. Bull*., *57*, 133-150.
[17] Unwin, N. **(2000)** *Phil. Trans. R. Soc. Lond. B, 355*, 1813-1829.
[18] Unwin, N. **(2005)** *J. Mol. Biol*., *346*, 967-989.
[19] Arias, H.R. **(1998)** Biochim. Biophys. Acta Rev. Biomembr., 1376, 173-220.
[20] Arias, H.R. **(2001)** in *Drug-Receptor Thermodynamics: Introduction and Applications* (Raffa, R.B., Ed.). pp. 293-358. John Wiley & Sons, Ltd., USA.
[21] Corringer, P.J., Le Novére, N. and Changeux, J-P. **(2000)** *Annu. Rev. Pharmacol. Toxicol*., *40*, 431-458.
[22] Sher, E., Chen, Y, Sharples, T.J., Broad, L.M., Benedetti, G., Zwart, R, McPhie, G.I., Pearson, K.H., Baldwinson, T. and De Filippi, G. **(2004)** *Curr. Top. Med. Chem*., *4*, 283-97.
[23] Gotti, C. and Clementi, F. **(2004)** *Prog. Neurobiol*., *74*, 363-96.
[24] Leonard, S. and Bertrand, D. **(2001)** *Nicot. Tobacco Res*., *3*, 203-223.
[25] Jones, M.V. and Westbrook, G.L. **(1996)** *Trends Neurosci., 19*, 96-101.
[26] Dilger, J.P. and Vidal, A.M. **(1994)** *Mol. Pharmacol*., *46*, 169-175.
[27] Dilger, J.P., Brett, R.S. and Mody, H.I. **(1993)** *Mol. Pharmacol*., *44*, 1056-1063.

[28] Dilger, J.P., Liu, Y. and Vidal, A.M. **(1995)** *Eur. J. Anaesthesiol. 12*, 31-39.
[29] Wenningmann, I., Barann, M., Vidal, A.M. and Dilger, J.P. **(2001)** *Mol. Pharmacol., 60*, 584-594.
[30] Scheller, M., Buffler, J., Schneck, H., Kochs, E. and Franke, C. **(1997)** *Anesthesiology, 86*, 118-127.
[31] Violet, J.M., Downie, D.L., Nakisa, R.C., Lieb, W.R. and Franks, N.P. **(1997)** *Anesthesiology, 86*, 866-874.
[32] Raines, D.E., Rankin, S.E. and Miller, K.W. **(1995)** *Anesthesiology* 82, 276-287.
[33] Pocock, G. and Richards, C.D. **(1988)** *Br. J. Pharmacol., 95*, 209-217.
[34] McKenzie, D., Franks, N.P. and Lieb, W.R. **(1995)** *Br. J. Pharmacol., 115*, 275-282.
[35] Eger 2nd , E.I., Koblin, D.D., Harris, R.A., Kendig, J.J., Pohorille, A., Halsey, M.J. and Trudell, J.R. **(1997)** *Anesth. Analg., 84*, 915-918.
[36] Cardoso, R.A., Yamakura, T., Brozowski, S.J., Chavez-Noriega, L.E. and Harris, R.A. **(1999)** *Anesthesiology, 91*, 1370-1377.
[37] Mori, T., Zhao, X., Zuo, Y., Aistrup, G.L., Nishikawa, K., Marszalec, W., Yeh, J.Z. and Narahashi, T. **(2001)** *Mol. Pharmacol., 59*, 732-743.
[38] Downie, D.L., Vicente-Agulló, F., Campos-Caro, A., Bushell, T.J., Lieb, W.R. and Franks, N.P. **(2002)** *J. Biol. Chem., 277*, 10367-10373.
[39] Zhang, L., Oz, M., Stewart, R.R., Peoples, R.W. and Weight, F.F. **(1997)** *Br. J. Pharmacol., 120*, 353-355.
[40] Yu, D., Zhang, L., Eiselé, J.L., Bertrand, D. and Changeux, J-P. **(1996)** *Mol. Pharmacol., 50*, 1010-1016.
[41] Forman, S.A., Miller, K.W. and Yellen, G. **(1995)** *Mol. Pharmacol., 48*, 574-581.
[42] Barann, M., Wenningmann, I. and Dilger, J.P. **(1998)** *Toxicol. Lett., 100-101*, 155-161.
[43] Yamakura, T., Borghese, C. and Harris, A. **(2000)** *J. Biol. Chem., 275*, 40879-40886.
[44] Eckenhoff, R.G. **(1996)** *Proc. Natl. Acad. Sci. USA, 93*, 2807-2810.
[45] Xu, Y., Seto, T., Tang, P. and Firestone, L.O. **(2000)** *Biophys. J., 78***,** 746-751.
[46] Seto, T. and Firestone, L.L. **(2000)** *Biochim. Biophys. Acta, 1509*, 111-122.
[47] Eckenhoff, M.F., Chan, K. and Eckenhoff, R.G. **(2002)** *J. Pharm. Exp. Ther., 300*, 172-179.
[48] Ziebell, M.R., Nirthanan, S., Husain, S.S., Miller, K.W. and Cohen, J.B. **(2004)** *J. Biol. Chem., 279*, 17640-17649.
[49] Krasowski, M.D. and Harrison, N.L. **(1999)** *Cell Mol. Life Sci., 55*, 1278-128.
[50] Murrell, R.D., Braun, M.S. and Haydon, D.A. **(1991)** *J. Physiol., 437*, 431-448.
[51] Wood, S.C., Forman, S.A. and Miller, K.W. **(1991)** *Mol. Pharmacol., 39*, 332-338.
[52] Godden, E.L., Harris, R.A. and Dunwiddie, T.V. **(2001)** *J. Pharmacol. Exp. Ther., 296*, 716-722.
[53] Zuo, Y., Aistrup, G.L., Marszalec, W., Gillespie, A., Chavez-Noriega, L.E., Yeh, J.Z. and Narahashi, T. **(2001)** *Mol. Pharmacol., 60*, 700-711.
[54] Godden, E.L. and Dunwiddie, T.V. **(2002)** *Alcohol. Clin. Exp. Res., 26*, 8-18.
[55] Wood, S.C., Hill, W.A. and Miller, K.W. **(1993)** *Mol. Pharmacol., 44*, 1219-1226.
[56] Wood, S.C., Tonner, P.H., de Armendi, A.J., Bugge, B. and Miller, K.W. **(1995)** *Mol. Pharmacol., 47*, 121-130.
[57] Campagna, J.A., Miller, K.A. and Forman, S.A. **(2003)** *N. Engl. J. Med., 348*, 2110-2124.
[58] Pratt, M.B., Husain, S.S., Miller, K.W. and Cohen, J.B. **(2000)** *J. Biol. Chem., 275*, 29441-294.
[59] Mascia, M.P., Trudell, J.R. and Harris, R.A. **(2000)** *Proc. Natl. Acad. Scil. USA, 97*, 9305-9310.
[60] Forman, S.A. and Zhou, Q. **(1999)** *Mol. Pharmacol., 55*, 102-108.
[61] Aistrup, G.L., Marszalec, W. and Narahashi, T. **(1999)** *Mol. Pharmacol., 55*, 39-49.
[62] Cardoso, R.A., Brozowski, S.J., Chavez-Noriega, L.E., Harpold, M., Valenzuela, F.C. and Harris, R.A. **(1999a)** *J. Pharm. Exp. Ther., 289*, 774-780.
[63] Liu, Y., Dilger, J.P. and Vidal, A.M. **(1994)** *Mol. Pharmacol. 45*, 1235-1241.
[64] Raines, D.E., Claycomb, R.J., Scheller, M. and Forman, S.A. **(2001)** *Anesthesiology, 95*, 470- 477.
[65] Mascia, M.P., Maiya, R., Borghese, C.M., Lobo, I.A., Hara, K., Yamakura, T., Gong, D.H. and Beckstead, M.J. **(2001)** *Alcohol. Clin. Exp. Res., 25*, 1570-1575.
[66] Yamakura, T., Bertaccini, E., Trudell, J.R. and Harris, R.A. **(2001)** *Annu. Rev. Pharmacol. Toxicol., 41*, 23-51.
[67] Kamiya, Y. andoh, T., Watanabe, I., Higashi, T. and Itoh, H. **(2001)** *Anesthesiology, 94*, 694-704.
[68] Yamakura, T., Chavez-Noriega, L.E. and Harris, R.A. **(2000)** *Anesthesiology,* 92, 1144-1153.
[69] Arias, H.R., McCardy, E.A., Gallagher, M.J. and Blanton, M.P. **(2001)** *Mol. Pharmacol., 60*, 497-506.
[70] de Armendi, A.J., Tonner, P.H., Bugge, B. and Miller, K.W. **(1993)** *Anesthesiology, 79*, 1033-1041.
[71] Arias, H.R., Kem, W.R., Trudell, J.R. and Blanton, M.P. **(2002)** *Int. Rev. Neurobiol., 54*, 1-50.
[72] Tonner, P.H. and Miller, K.W. **(1995)**. *Eur. J. Anaesthesiol., 12*, 21-30.
[73] Coates, K.M., Mather, L.E., Johnson, R. and Flood, P. **(2001)** *Anesth. Analg., 92*, 930-933.
[74] Sumikawa, K., Matsumoto, T., Amenomori, Y., Hirano, H. and Amakata, Y. **(1983)** *Anesthesiology, 59*, 412-416.
[75] Andoh, T., Furuya, R., Oka, K., Hattori, S., Watanabe, I., Kamiya, Y. and Okumura, F. **(1997)** *Anesthesiology, 87*, 1199-1209.
[76] Dilger, J.P., Boguslavsky, R., Barann, M., Katz, T. and Vidal, A.M. **(1997)** *J. Gen. Physiol., 109*, 401-414.
[77] Downie, D.L., Franks, N.P. and Lieb, W.R. **(2000)** *Anesthesiology, 93*, 774-783.
[78] Watanabe, I. andoh, T., Furuya, R., Sasaki, T., Kamiya, Y. and Itoh, H. **(1999)** *Anesth. Analg., 88*, 1406-1411.
[79] Dodson, B.A., Urh, R.R. and Miller, K.W. **(1990)** *Br. J. Pharmacol., 101*, 710-714.
[80] Blanton, M.P., McCardy, E.A. and Gallagher, M.J. **(2000)** *J. Biol. Chem., 275*, 3469-3478.
[81] Gallagher, M.J. and Cohen, J.B. **(1999)** *Mol. Pharmacol., 56*, 300-307.
[82] White, B.H. and Cohen, J.B. **(1992)** *J. Biol. Chem., 267*, 15770-15783.
[83] Yost, C.S. and Dodson, B.A. **(1993)** *Cell. Mol. Neurobiol., 13*, 159-172.
[84] Buisson, B. and Bertrand, D. **(1998)** *Mol. Pharmacol., 53*, 555-563.
[85] Grewer, C. and Hess, G.P. **(1999)** *Biochemistry, 38*, 7837-7846.
[86] Briggs, C.A. and McKenna, D.G. **(1996)** *Neuropharmacology, 35*, 407-414.
[87] Arias, H.R., McCardy, E.A. and Blanton, M.P. **(2001)** *Mol. Pharmacol.,* 59, 1051-1060.
[88] Amador, M. and Dani, J.A. **(1991)** *Synapse, 7*, 207-215.
[89] Ramoa, A.S., Alkondon, M., Aracava, Y., Irons, J., Lunt, G.G., Deshpande, S.S., Wonnacott, S., Aronstam, R.S. and Alburquerque, E.X. **(1990)** *J. Pharmacol. Exp. Ther., 254*, 71-82.
[90] Herz, J.M., Johnson, D.A. and Taylor, P. **(1989)** *J. Biol. Chem., 262*, 12439-12448.
[91] Pratt, M.B., Pedersen, S.E. and Cohen, J.B. **(2000)** *Biochemistry, 39*, 11452-11462.
[92] Lurtz, M.M. and Pedersen, S.E. **(1999)** *Mol. Pharmacol., 55***,** 159-167.
[93] Bencherif, M., Eisenhour, C.M., Prince, R.J., Lippiello, P.M. and Lukas, R.J. **(1995)** *J. Pharmacol. Exp. Ther., 275*, 1418-1426.
[94] Sun, H., McCardy, E.A., Machu, T.K. and Blanton, M.P. **(1999)** *J. Pharmacol. Exp. Ther., 290*, 129-135.
[95] Arias, H.R., Valenzuela, C.F. and Johnson, D.A. **(1993)** *Biochemistry, 32*, 6237-6242.
[96] Arias, H.R. **(1997)** *Biochim. Biophys. Acta, 1347*, 9-22.
[97] Arias, H.R., Valenzuela, C.F. and Johnson, D.A. **(1993)** *J. Biol. Chem., 268*, 6348-6355.
[98] Arias, H.R. **(1999)** *Arch. Biochem. Biophys. 371*, 89-97.
[99] Blanton, M.P., McCardy, E.A., Huggins, A. and Parikh, D. **(1998)** *Biochemistry, 37*, 14545-14555.
[100] DiPaola, M., Kao, P.N. and Karlin, A. **(1990)** *J. Biol. Chem., 265*, 11017-11029.
[101] Tamamizu, S., Todd, A.P. and McNamee, M.G. **(1995)** *Cell Mol. Neurobiol., 15*, 427-438.
[102] Hess, G.P., Ulrich, H., Breitinger, H.G., Niu, L., Gameiro, A.M., Grewer, C., Srivastava, S., Ippolito, J.E., Lee, S.M., Jayaraman, V.

and Coombs, S.E. **(2000)** *Proc. Natl. Acad. Sci. USA, 97*, 13895-13900.
[103] Halliwell, R.F., Peters, J.A. and Lambert, J.J. **(1989)** *Br. J. Pharmacol., 96*, 480-494.
[104] Connolly, J., Boulter, J. and Heinemann, S.F. **(1992)** *Br. J. Pharmacol., 105*, 657-666.
[105] Flood, P. and Krasowski, M.D. **(2000)** *Anesthesiology, 92*, 1418-1425.
[106] Mosckovitz, R., Haring, R., Gershoni, J.M., Kloog, Y. and Sokolovsky, M. **(1987)** *Biochem. Biophys. Res. Commun., 145*, 810-816.
[107] Eteroviç, V.A., Lu, R., Eakin, A.E., Rodríguez, A.D. and Ferchmin, P.A. **(1999)** *Cell Mol. Neurobiol., 19*, 745-757.
[108] Eaton, M.J., Labarca, C.G. and Eteroviç, V.A. **(2000)** *J. Neurosci. Res. 61*, 44-51.
[109] Volle, R.L., Alkadhi, K.A., Branisteanu, D.D., Reynolds, L.S., Epstein, P.M., Smilowitz, H., Lambert, J.J. and Henderson, E.G. **(1982)** *J. Pharm. Exp. Ther., 221*, 570-576.
[110] Arias, H.R., McCardy, E.A., Bayer, E.Z., Gallagher, M.J. and Blanton, M.P. **(2002)** *Arch. Biochem. Biophys., 403*, 121-131.
[111] Ryan, S.E., Blanton, M.P. and Baenziger, J.E. **(2001)** *J. Biol. Chem., 276*, 4796-4803.
[112] Gallagher, M.J., Chiara, D.C. and Cohen, J.B. **(2001)** *Mol. Pharmacol., 59*, 1514-1522.
[113] Middleton, R.E., Strnad, N.P. and Cohen, J.B. **(1999)** *Mol. Pharmacol.*, 56, 290-299.
[114] Arias, H.R., Trudell, J.R., Bayer E.Z., Hester, B., McCardy, E.A. and Blanton, M.B. **(2003)** *Biochemistry, 42*, 7358-7370.
[115] Sasaki, T. andoh, T., Watanabe, I., Kamiya, Y., Itoh, H., Higashi, T. and Matsuura, T. **(2000)** *Anesth. Analg., 91*, 741-748.
[116] Purifoy, J.A. and Holz, R.W. **(1984)** *Life Sci., 35*, 1851-1857.
[117] Friederich, P., Dybek, A. and Urban, B. **(2000)** *Anesthesiology, 93*, 818-824.
[118] Ryder, S., Way, W.L. and Trevor, A.J. **(1978)** *Eur. J. Pharmacol., 49*, 15-23.
[119] White, P.F., Schuttler, J., Shafer, A., Stanski, D.R., Horai, Y. and Trevor, A.J. **(1985)** *Br. J. Anaesth., 57*, 197-203.
[120] Lodge, D., Anis, N.A. and Burton, N.R. **(1982)** *Neurosci. Lett., 29*, 281-286.
[121] Dayton, P.G., Stiller, R.L., Cook, D.R. and Perel, J.M. **(1983)** *Eur. J. Clin. Pharmacol. 24*, 825-831.
[122] Koblin, D.D. and Lester, H. **(1979)** *Mol. Pharmacol., 15*, 559-580.
[123] Charnet, P., Labarca, C., Cohen, B.N., Davidson, N., Lester, H.A. and Pilar, G. (**1992)** *J. Physiol., 450*, 375-394.
[124] Cuevas, J. and Adams, D.J. **(1994)** *Br. J. Pharmacol., 111*, 663-672.
[125] Francis, M.M., Vazquez, R.W., Papke, R.L. and Oswald, R.E. (**2000)** *Mol. Pharmacol., 58*, 109-119.
[126] Adams, P.R. **(1977)** *J. Physiol., 268*, 291-318.
[127] Neher, E. and Steinbach, J.H. **(1978)** *J. Physiol., 277*, 153-176.
[128] Charnet, P., Labarca, C. and Lester, H.A. **(1994)** *Mol. Pharmacol., 41*, 708-717.
[129] Charnet, P., Labarca, C., Leonard, R.J., Vogelaar, N.J., Czyzyk, L., Gouin, A., Davidson, N. and Lester, H.A. **(1990)** *Neuron, 2*, 87-95.
[130] Leonard, R.J., Labarca, C.G., Charnet, P., Davidson, N. and Lester, H.A. **(1988)** *Science, 242*, 1578-1581.
[131] Horn, R., Brodwick, M.S. and Dickey, W.D. **(1980)** *Science, 210*, 205-207.
[132] Gage, P.W., Hamill, O.P. and Wachtel, R.E. **(1983)** *J. Physiol., 335*, 123-137.
[133] Swanson, K.L. and Alburquerque, E.X. **(1987)** *J. Pharmacol. Exp. Ther., 243*, 1202-1210.
[134] Aracava, Y., Ikeda, S.R., Daly, J.W., Brookes, N. and Alburquerque, E.X. (**1984)** *Mol. Pharmacol., 26*, 304.
[135] Ikeda, S.R., Aronstam, R.S., Daly, J.W., Aracava, Y. and Alburquerque, E.X. **(1984)** *Mol. Pharmacol., 26*, 293-303.
[136] Aguayo, L.G., Pazhenchevsky, B., Daly, J.W. and Alburquerque, E.X. **(1981)** *Mol. Pharmacol., 20*, 33-45.
[137] Niu, L. and Hess, G.P. **(1993)** *Biochemistry, 32*, 3831-3835.
[138] Niu, L., Abood, L.G. and Hess, G.P. **(1995)** *Proc. Natl. Acad. Sci., USA, 92*, 1208-12012.
[139] Horváth, L.I., Arias, H.R., Hankovszky, H.O., Hideg, K., Barrantes, F.J. and Marsh, D. **(1990)** *Biochemistry, 29*, 8707-8713.
[140] Mantipragada, S.B., Horváth, L.I., Arias, H.R., Schwarzmann, G., Sandhoff, K., Barrantes, F.J. and Marsh, D. **(2003)** *Biochemistry, 42*, 9167-9175.
[141] Heidmann, T., Oswald, R.E. and Changeux, J-P. **(1983)** *Biochemistry, 22*, 3112-3127.
[142] Oswald, R.E. and Changeux, J.-P. **(1981)** *Biochemistry, 20*, 7166-7174.
[143] Pedersen, S.E., Sharp, S.D., Liu, W.S. and Cohen, J.B. **(1992)** *J. Biol. Chem., 267*, 10489-10499.
[144] Bouzat, C. and Barrantes, F.J. **(1996)** *J. Biol. Chem., 271*, 25835-25841.
[145] Revah, F., Bertrand, D., Galzi, J.-L., Devillers-Thiéry, A., Mulle, C., Hussy, N., Bertrand, S., Ballivet, M. and Changeux, J.-P. **(1991)** *Nature, 353*, 846.
[146] Pascual, J.M. and Karlin, A. **(1998)** *J. Gen. Physiol., 111*, 717-739.
[147] Wilson, G.G. and Karlin, A. **(1998)** *Neuron, 20*, 1269-1281.
[148] Wilson, G.G. and Karlin, A. **(2001)** *Proc. Natl. Acad. Sci., USA, 98*, 1241-1248.
[149] Eteroviç, V.A., Li, L., Ferchmin, P.A., Lee, Y.H., Hann, R.M., Rodríguez, A.D. and McNamee M.G. **(1993)** *Cell. Mol. Neurobiol., 13*, 111-121.
[150] Flood, P., Ramirez-Latorre, J. and Role, L. **(1997)** *Anesthesiology, 86*, 859-865.
[151] Dodson, B.A., Braswell, L.M. and Miller, K.W. **(1987)** *Mol. Pharmacol., 32*, 119-126.
[152] Roth, S.H., Forman, S.A., Braswell, L.M. and Miller, K.W. **(1989)** *Mol. Pharmacol., 36*, 874-880.
[153] Herz, J.M., Johnson, D.A. and Taylor, P. **(1987)** *J Biol Chem., 262*, 7238-7247
[154] Karpen, J.W. and Hess, G.P. **(1986)** *Biochemistry, 25*, 1777-1785.
[155] Karpen, J.W., Aoshima, H., Abood, L.G. and Hess, G.P. **(1982)** *Proc. Natl. Acad. Sci. USA, 79*, 2509-2513.
[156] Pagán, O.R., Eteroviç, V.A., Garcia, M., Vergne, D., Basilio, C.M., Rodríguez, A.D. and Hann, R.M. **(2001)** *Biochemistry, 40*, 11121-11130.
[157] Aronstam, R.S., Narayanan, L. and Wenger, D.A. **(1982)** *Eur. J. Pharmacol, 78*, 367-370.
[158] Scheller, M., Bufler, J., Hertle, I., Schneck, H.J., Franke, C. and Kochs, E. **(1996)** *Anesth. Analg., 83*, 830-836.
[159] Coates, K.M. and Flood, P. **(2001)** *Br J Pharmacol., 134*, 871-879
[160] Aronstam, R.S., Eldefrawi, A.T., Pessah, I.N. and Daly, J.W. **(1981)** *J. Biol. Chem., 256*, 2843.
[161] Bufler, J., Franke, C., Parnas, H. and Dudel, J. **(1996)** *Eur. J. Neurosci., 8*, 677-687.
[162] Dudel, J., Schramm, M., Franke, C., Ratner, E. and Partnas, H. **(1999)** *J. Neurophysiol., 81*, 2386-2397.
[163] Charlesworth, P., Jacobson, I, Pocock, G. and Richards, C.D. **(1992)** *Br. J. Pharmacol., 106*, 802-812.
[164] Damaj, M.I., Slemmer, J.E., Carroll, F.I. and Martin, B.R. **(1999)** *J. Pharmacol. Exp. Ther., 289*, 1229-1236.
[165] Hennings, E.C, Kiss, J.P., De Oliveira, K., Toth, P.T. and Vizi, E.S. **(1999)** *J. Neurochem., 73*, 1043-1050.
[166] Ogden, D.C., Siegelbaum, S.A. and Colquhoun, D. **(1981)** *Nature, 289*, 596-598.
[167] Weiland, G.A., Durkin, J.A., Henley, J.M. and Simasko, S.M. **(1987)** *Mol. Pharmacol., 32*, 625-632.
[168] Neher, E. **(1983)** *J. Physiol., 339*, 663-678.
[169] Ruff, R.L. **(1982)** *Biophys. J., 37*, 625-631.
[170] Palma, A., Herz, J.M., Wang, H.H. and Taylor, P. **(1986)** *Mol. Pharmacol., 30*, 243-251.
[171] Dreyer, E.B., Hasan, F., Cohen, S.G. and Cohen, J.B. **(1986)** *J. Biol. Chem., 261*, 13727-13734.
[172] Boyd, N.D. and Cohen, J.B. **(1984)** *Biochemistry, 23*, 4023-4033.
[173] Lin, L., Koblin, D.D. and Wang, H.H. (1995) *Biochem. Pharmacol., 49*, 1085-1089.
[174] Katz, E.J., Cortes, V.I., Eldefrawi, M.E. and Eldefrawi, A.T. **(1997)** *Toxicol. Appl. Pharmacol., 146*, 227-236.
[175] Furuya, R., Oka, K., Watanabe, I., Kamiya, Y., Itoh, H. and Andoh, T. **(1999)** *Anesth. Analg., 88*, 174-180.

Received: March 30, 2005 Accepted: July 15, 2005